Recent advances in the description of lepton-nucleus scattering

Noemi Rocco

Uncertainty Quantification in Nuclear Physics
MITP— June 24 - 28, 2024

Outline

- Lepton - nucleus interactions : GFMC
- Lepton - nucleus interactions : Factorization Scheme
- Lepton - nucleus interactions : BSM scenarios
  - Bayesian Artificial Neural network

Noemi Rocco, nrocco@fnal.gov

Addressing Neutrino-Oscillation Physics

$$P_{\nu_\mu \to \nu_e}(E, L) \sim \sin^2 2\theta \sin^2 \left(\frac{\Delta m^2 L}{4E}\right) \to \Phi_e(E, L)/\Phi_\mu(E, 0)$$

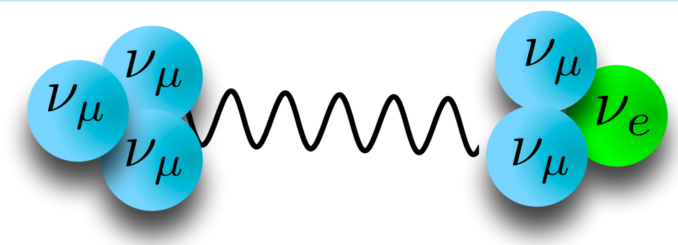

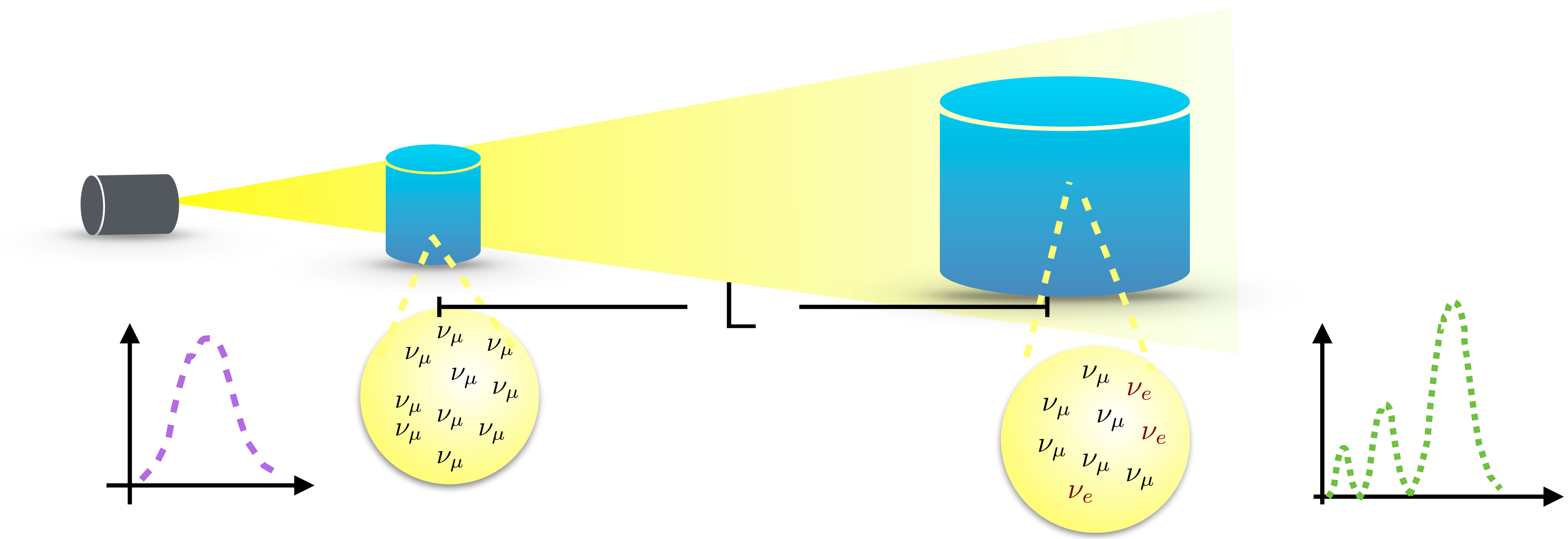

Detectors measure the **neutrino interaction rate:**

$$N_e(E_{\rm rec}, L) \propto \sum_i \Phi_e(E, L)\sigma_i(E) f_{\sigma_i}(E, E_{\rm rec}) dE$$

Reconstructed ν energy

Cross Section

Smearing matrix

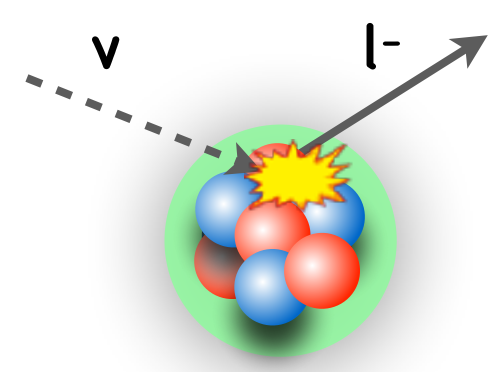

A precise determination of σ(E) is crucial to extract ν oscillation parameters

Noemi Rocco, nrocco@fnal.gov

Inputs for the nuclear model

Unprecedented accuracy in the determination of **neutrino-argon cross section** is required to achieve design sensitivity to CP violation at DUNE

More than 60% of the interactions at DUNE are non-quasielastic

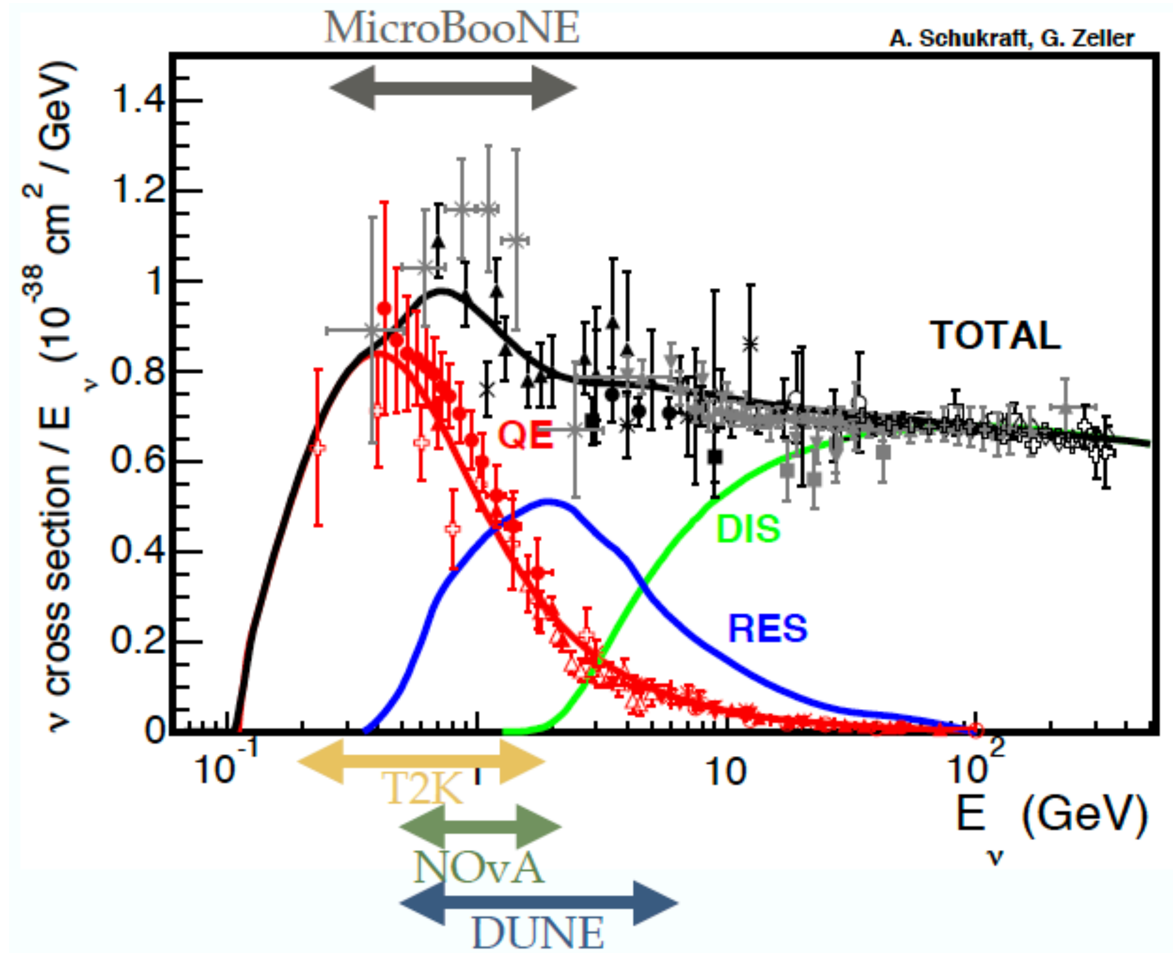

Theoretical tools for neutrino scattering,
Contribution to: 2022 Snowmass Summer Study

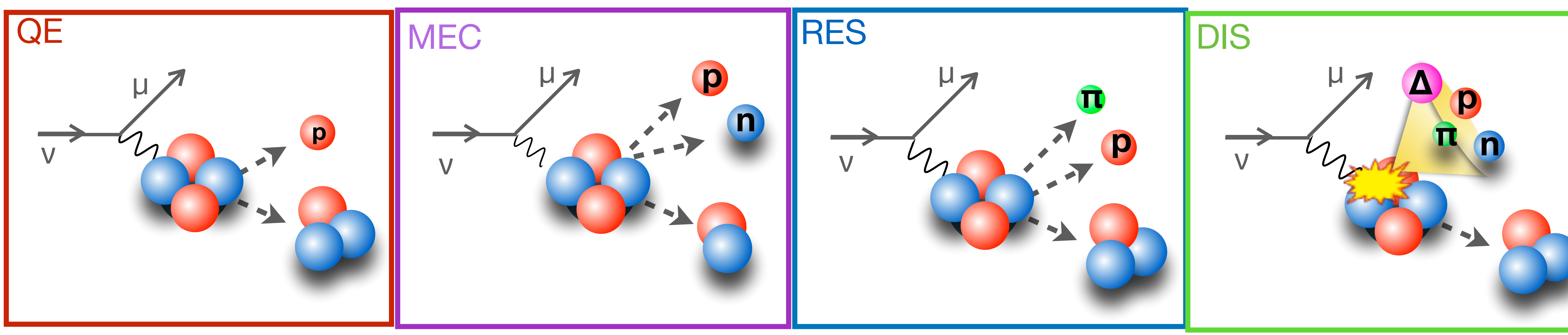

Why do we need more precision?

CLAS and e4v collaboration,
Nature 599 (2021) 7886, 565-570

Used semi-exclusive electron scattering data to test models and event generators used in oscillation analyses

The results indicate the **need** for **substantial improvement** in the **accuracy** of the neutrino interactions' models and simulations

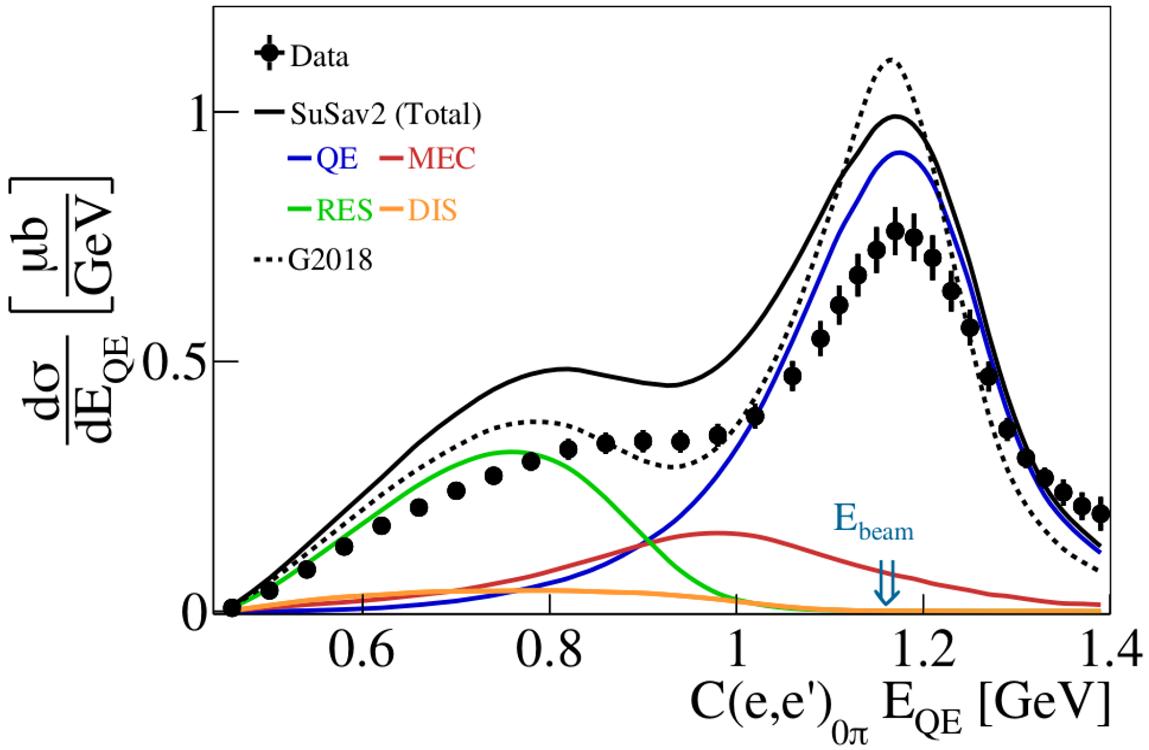

Current oscillation experiments report **large systematic uncertainties** associated with neutrino- nucleus interaction models.

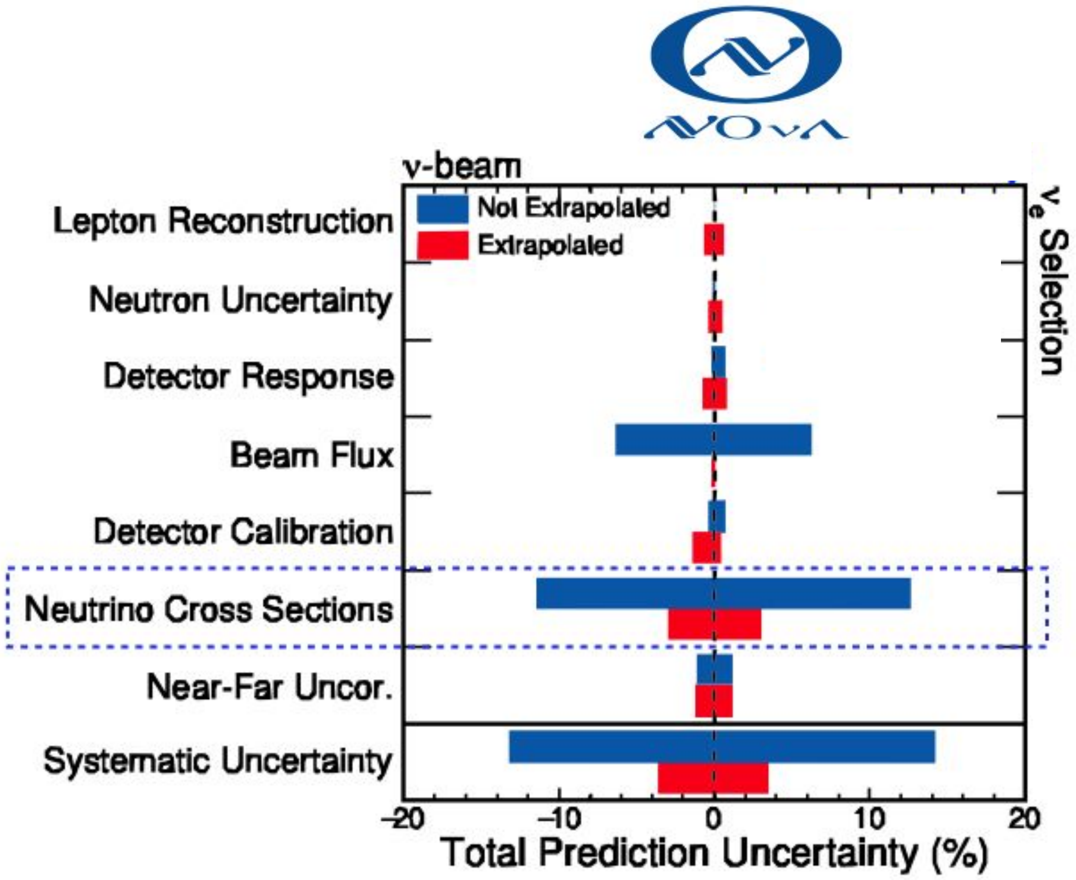

Noemi Rocco, nrocco@fnal.gov

Tuning

Discrepancies between generators and data often corrected by tuning an empirical model of the least well known mechanism: MEC ("meson exchange"/two-body currents)

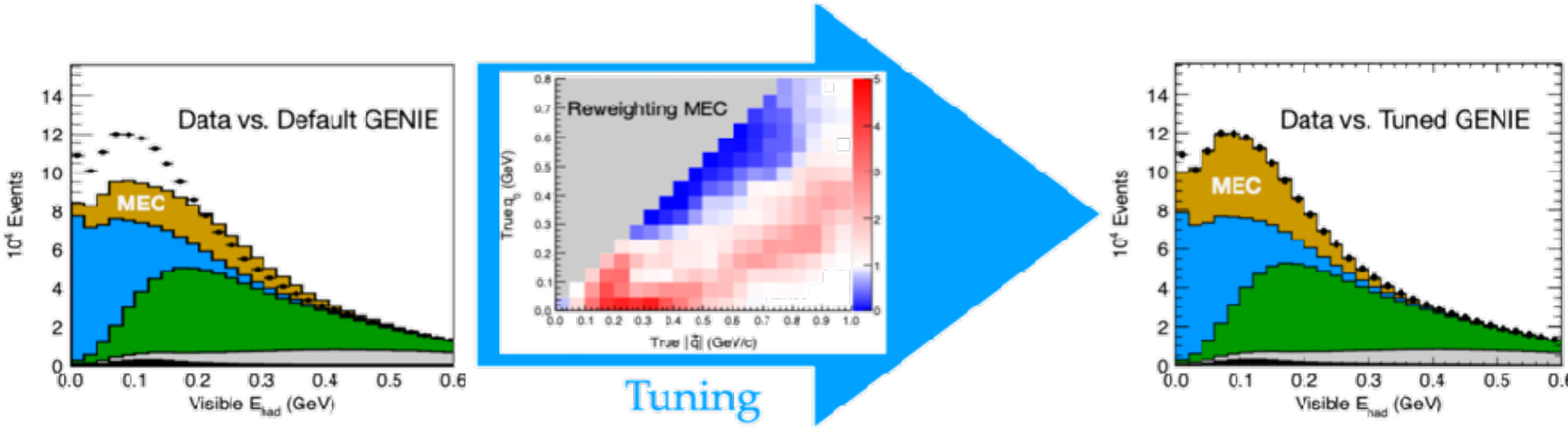

Coyle, Li, and Machado, JHEP 12, 166 (2022)

Mis-modeling can distort signals of new physics, **biasing** measurement of **new physics parameters**

Studies on the impact of different neutrino interactions and nuclear models on determining neutrino oscillation parameters are critical. These enable us to assess the level of precision we aim at.

Coloma, et al, Phys.Rev.D 89 (2014) 7, 073015

Noemi Rocco, nrocco@fnal.gov

Theory of lepton-nucleus scattering

- The cross section of the process in which a lepton scatters off a nucleus is given by

$$d\sigma \propto L^{\alpha\beta} R_{\alpha\beta}$$

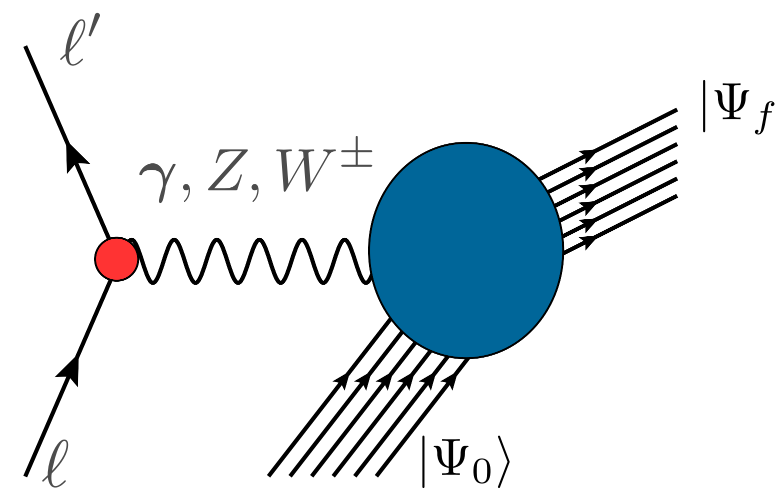

Leptonic Tensor: determined by lepton kinematics

Hadronic Tensor: nuclear response function

$$R_{\alpha\beta}(\omega, \mathbf{q}) = \sum_f \langle 0|J^\dagger_\alpha(\mathbf{q})|f\rangle\langle f|J_\beta(\mathbf{q})|0\rangle\delta(\omega - E_f + E_0)$$

The initial and final wave functions describe many-body states:

$$|0\rangle = |\Psi_0^A\rangle \ , |f\rangle = |\Psi_f^A\rangle, |\psi_p^N, \Psi_f^{A-1}\rangle, |\psi_k^\pi, \psi_p^N, \Psi_f^{A-1}\rangle \ldots$$

One and two-body current operators

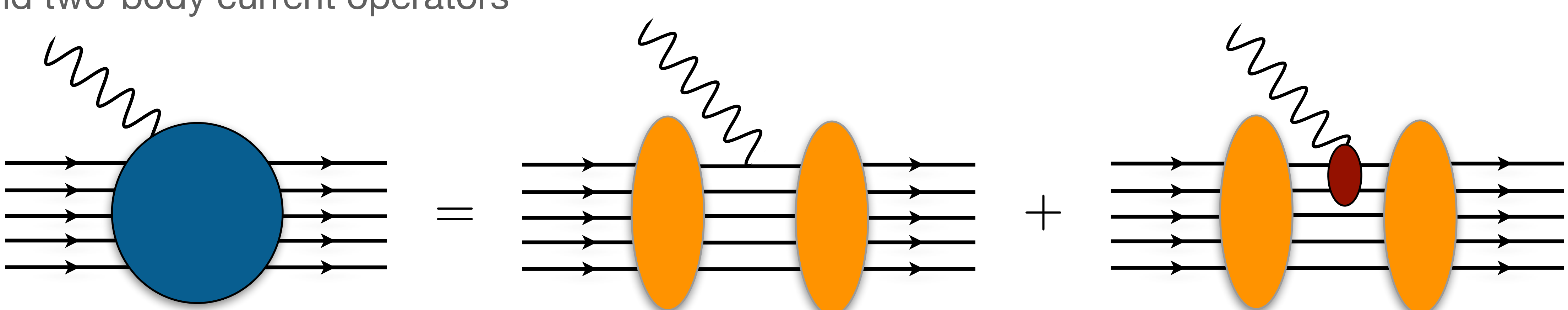

Ab initio Methods

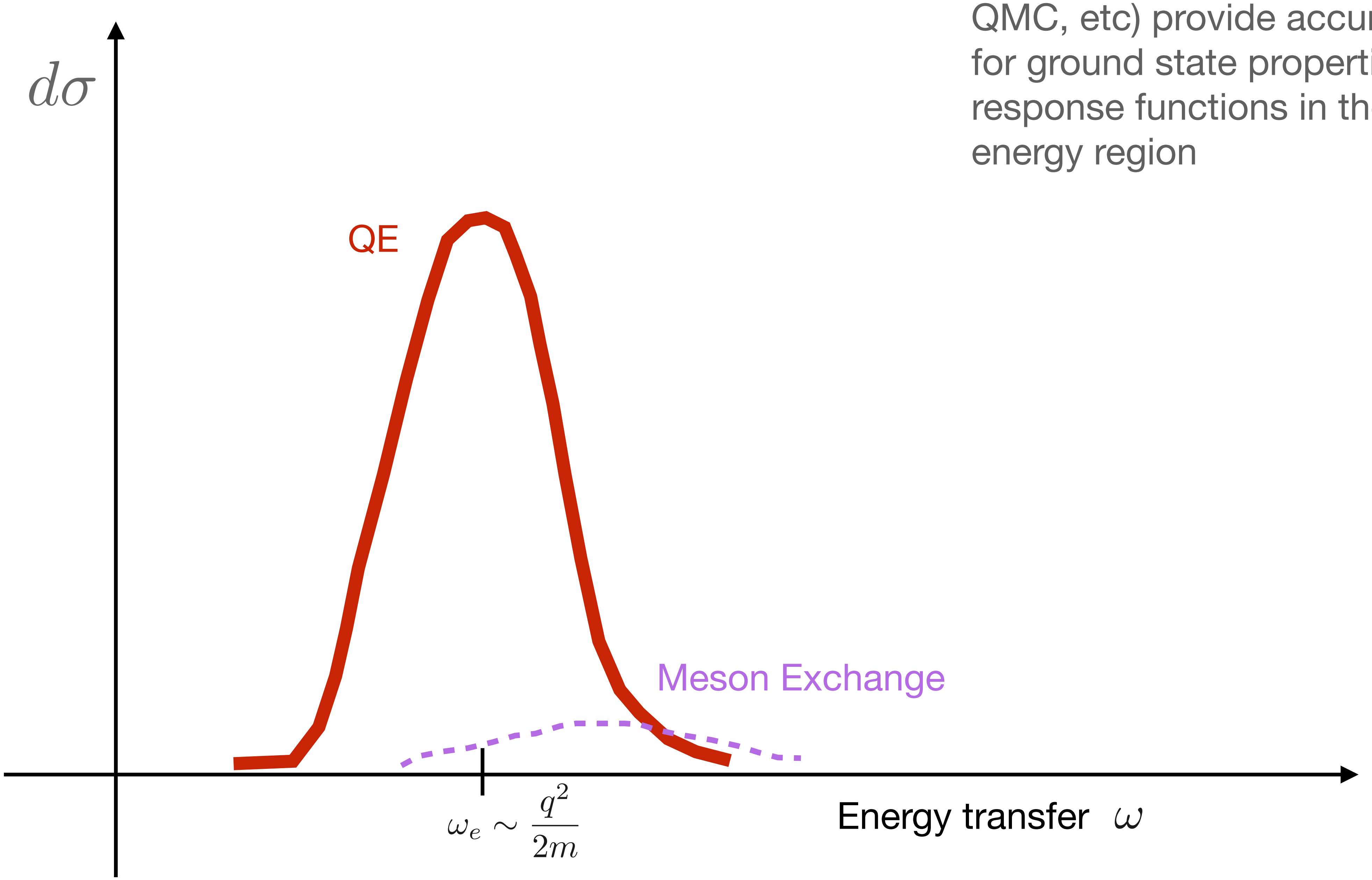

Ab-initio methods (CC, IMSRG, SCGF, QMC, etc) provide accurate predictions for ground state properties of nuclei + response functions in the low/moderate energy region

Noemi Rocco, nrocco@fnal.gov

Many-Body method: GFMC

QMC techniques **projects out the exact lowest-energy state:** $e^{-(H-E_0)\tau}|\Psi_T\rangle \rightarrow |\Psi_0\rangle$

Nuclear response function involves evaluating a number of transition amplitudes.
Valuable information can be obtained from the **integral transform of the response function**

$$E_{\alpha\beta}(\sigma,\mathbf{q}) = \int d\omega K(\sigma,\omega) R_{\alpha\beta}(\omega,\mathbf{q}) = \langle\psi_0|J^\dagger_\alpha(\mathbf{q}) K(\sigma, H-E_0) J_\beta(\mathbf{q})|\psi_0\rangle$$

Inverting the Laplace transform is a complicated problem

A. Lovato et al, PRL117 (2016), 082501, PRC97 (2018), 022502

— electron-^{4}He scattering

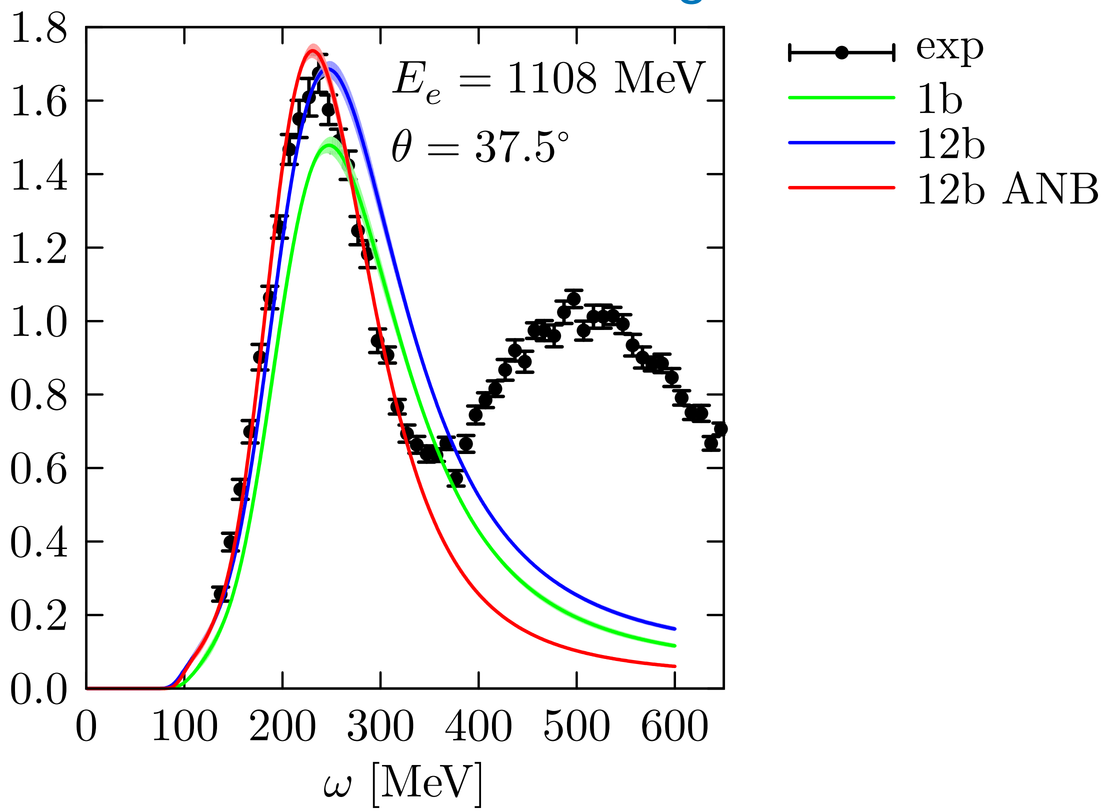

Inclusive results which are virtually correct in the QE

Different Hamiltonians can be used in the time-evolution operator

Relies on non-relativistic treatment of the kinematics

Can not handle explicit pion degrees of freedom

Noemi Rocco, nrocco@fnal.gov

Axial form factor determination

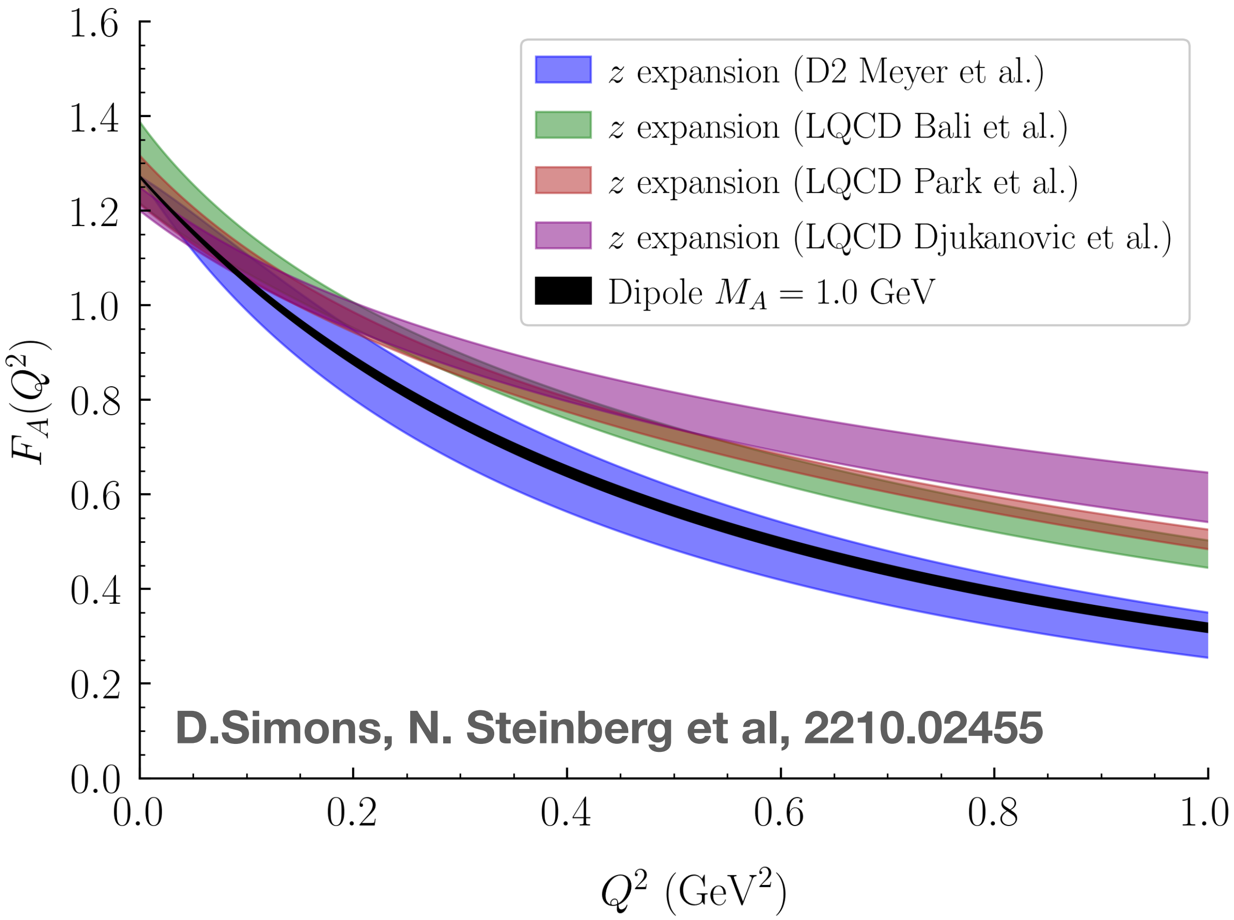

A. Meyer, A. Walker-Loud, C. Wilkinson, 2201.01839

D2 Meyer et al: fits to neutrino-deuteron scattering data

LQCD result: general agreement between the different calculations

LQCD results are 2-3σ larger than D2 Meyer ones for $Q^2 > 0.3$ GeV^2

Comparison with recent MINERvA antineutrino-hydrogen charged-current measurements

1-2σ agreement with MINERvA data and LQCD prediction by PNDME Collaboration

Novel methods are needed to remove excited-state contributions and discretization errors

O. Tomalak, R. Gupta, T. Battacharaya, 2307.14920

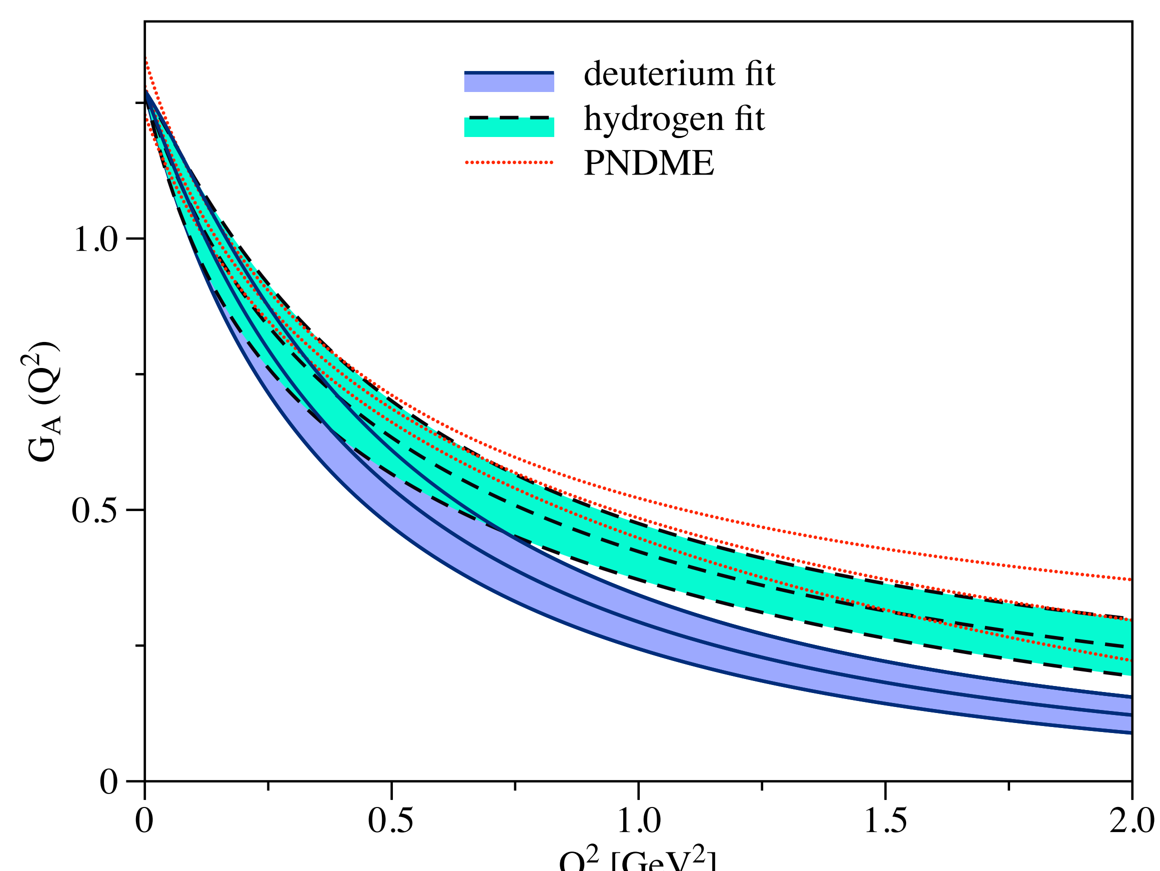

Noemi Rocco, nrocco@fnal.gov

Study of model dependence in neutrino predictions

MiniBooNE results; study of the dependence on the axial form factor:

D.Simons, N. Steinberg, NR, et al arXiv:2210.02455

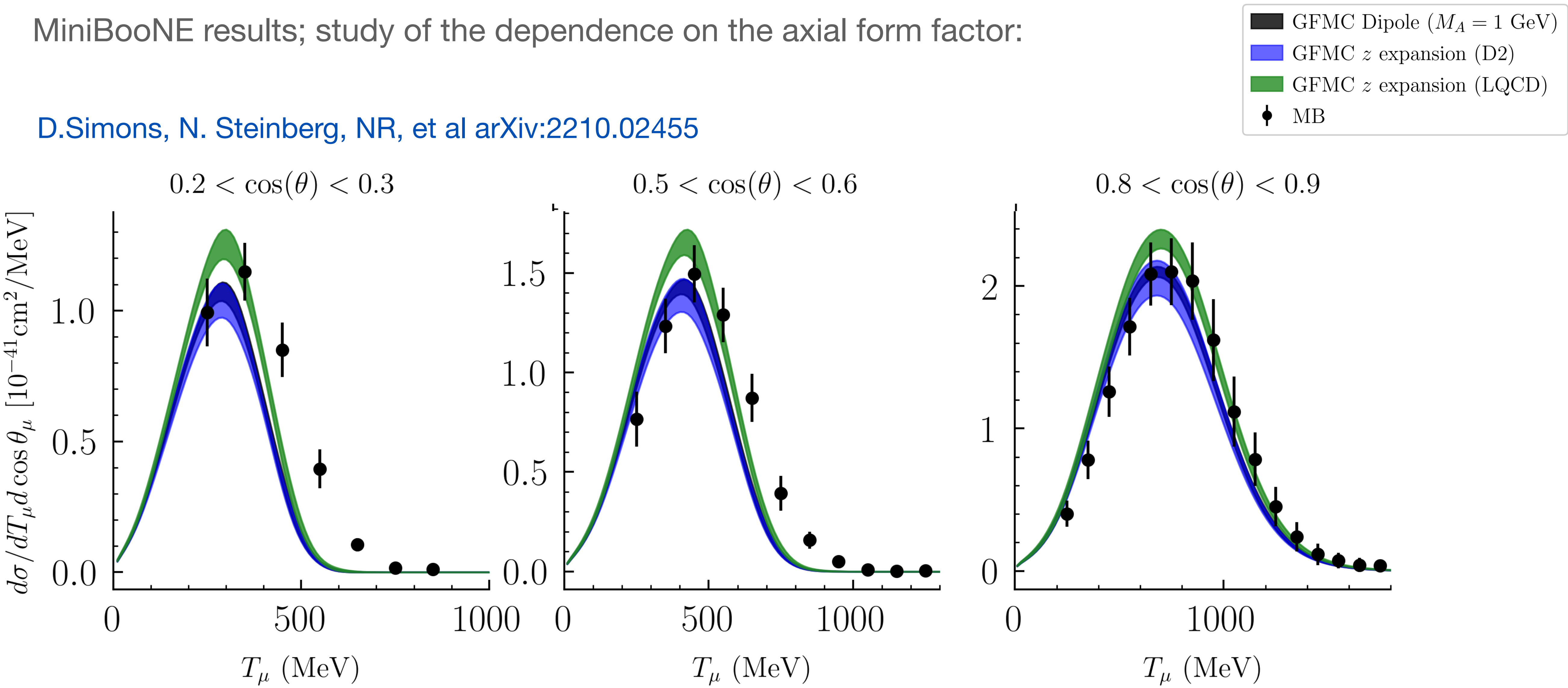

D.Simons, N. Steinberg et al, 2210.02455

MiniBooNE	$0.2 < \cos\theta_\mu < 0.3$	$0.5 < \cos\theta_\mu < 0.6$	$0.8 < \cos\theta_\mu < 0.9$
GFMC Difference in $d\sigma_{\text{peak}}$ (%)	18.6	17.1	12.2

Noemi Rocco, nrocco@fnal.gov

Study of model dependence in neutrino predictions

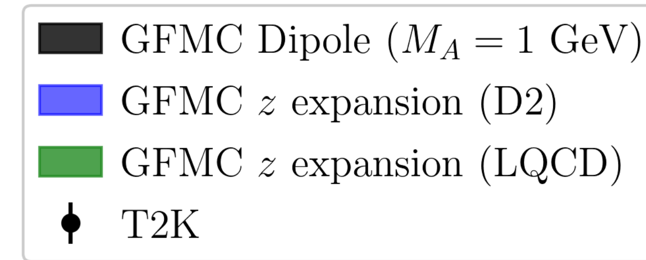

T2K results; study of the dependence on the axial form factor:

D.Simons, N. Steinberg, NR, et al arXiv:2210.02455

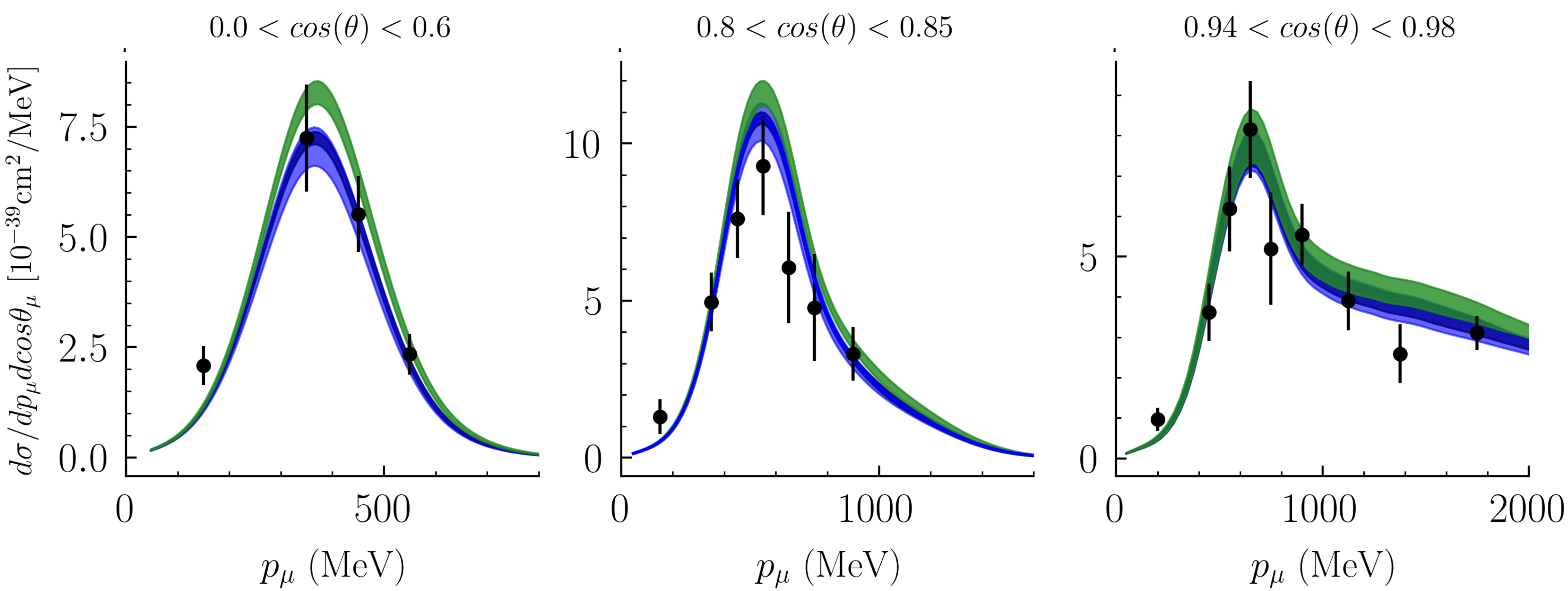

D.Simons, N. Steinberg et al, 2210.02455

T2K	$0.0 < \cos\theta_\mu < 0.6$	$0.80 < \cos\theta_\mu < 0.85$	$0.94 < \cos\theta_\mu < 0.98$
GFMC difference in $d\sigma_{\text{peak}}$ (%)	15.8	8.0	4.6

Noemi Rocco, nrocco@fnal.gov

Fermilab

Why relativity is important

$$R_{\alpha\beta}(\omega,\mathbf{q}) = \sum_f \underbrace{\langle 0|J_\alpha^\dagger(\mathbf{q})|f\rangle\langle f|J_\beta(\mathbf{q})|0\rangle}_{\text{Currents}}\underbrace{\delta(\omega - E_f + E_0)}_{\text{Kinematics}}$$

Covariant expression of the e.m. current:

$$j^\mu_{\gamma,S} = \bar{u}(\mathbf{p}')\Big[\frac{G_E^S + \tau G_M^S}{2(1+\tau)}\gamma^\mu + i\frac{\sigma^{\mu\nu}q_\nu}{4m_N}\frac{G_M^S - G_E^S}{1+\tau}\Big]u(\mathbf{p})$$

Nonrelativistic expansion in powers of $\boldsymbol{p}/m_N$

$$j^0_{\gamma,S} = \frac{G_E^S}{2\sqrt{1+Q^2/4m_N^2}} - i\frac{2G_M^S - G_E^S}{8m_N^2}\mathbf{q}\cdot(\boldsymbol{\sigma}\times\mathbf{p})$$

Energy transfer at the quasi-elastic peak:

$$w_{QE} = \sqrt{\mathbf{q}^2 + m_N^2} - m_N \qquad w_{QE}^{nr} = \mathbf{q}^2/(2m_N)$$

Noemi Rocco, nrocco@fnal.gov

Frame dependence

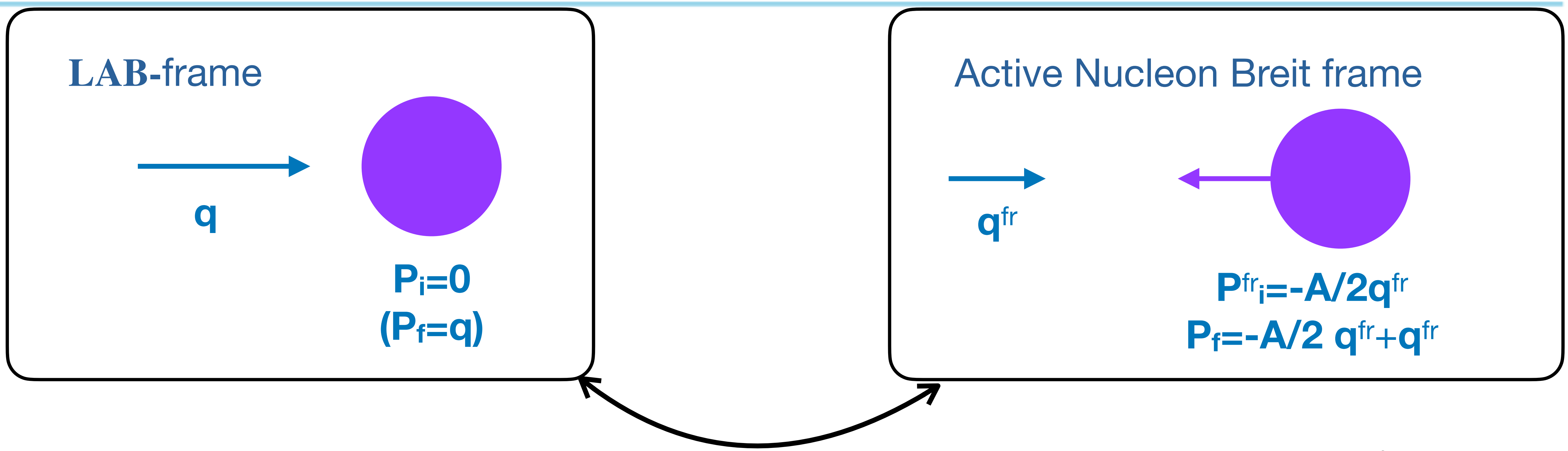

Lorentz Boost connects the two frames:

$$R^{\mu\nu}_{LAB}(\omega,q) = B^{\mu}{}_{\alpha}\,[\beta]\,B^{\nu}{}_{\beta}\,[\beta]\,R^{\alpha\beta}_{fr}(\omega^{fr},\mathbf{q}^{fr})$$

- LAB (solid) and ANB (dashed) predictions

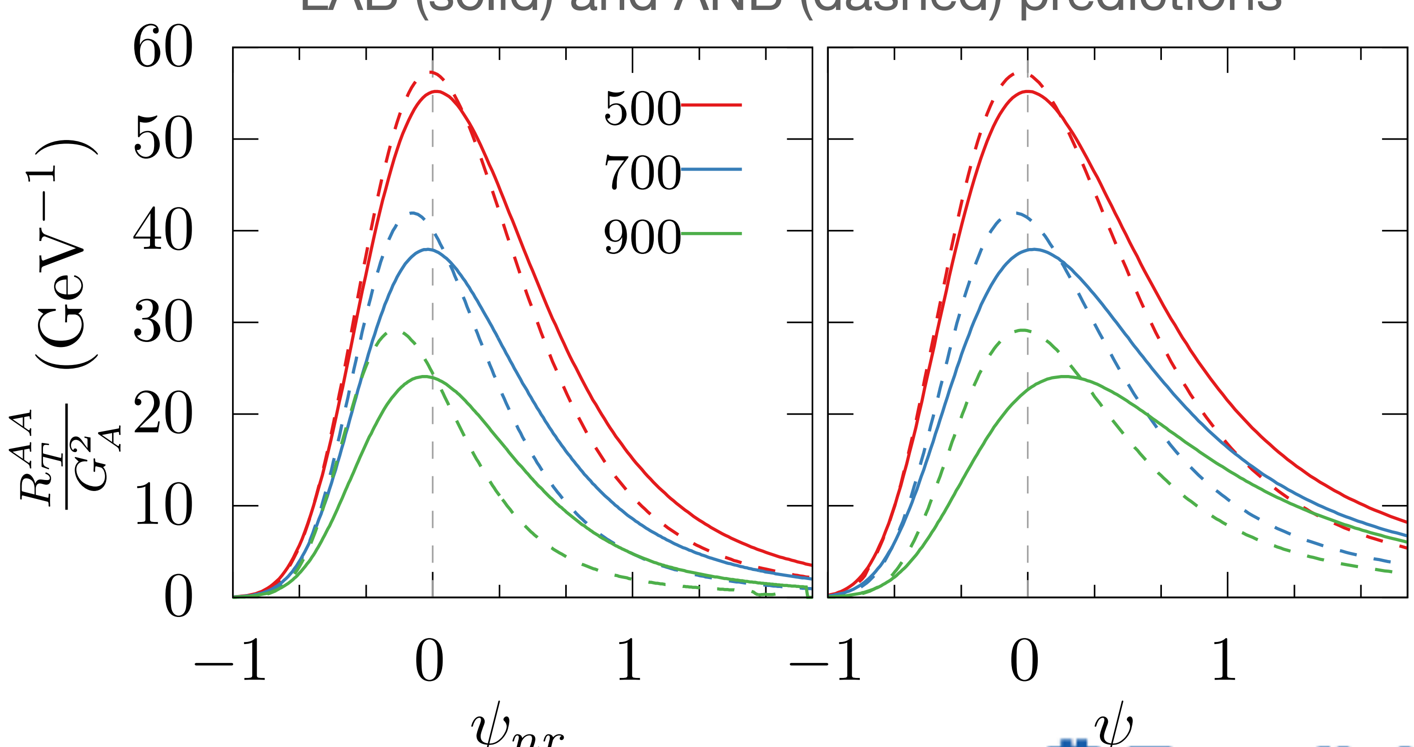

- ANB @ the single nucleon level:

  $p^{fr}_i \simeq -q^{fr}/2$

  $p^{fr}_f \simeq q^{fr}/2$

- Same position of the quasielastic peak

$$\omega_{QE} = \omega^{nr}_{QE} = 0$$

Noemi Rocco, nrocco@fnal.gov
Fermilab

Cross sections: Green's Function Monte Carlo

MiniBooNE results including relativistic corrections

A.Nikolakopoulos, A.Lovato, NR, PRC 109 (2024) 1, 014623

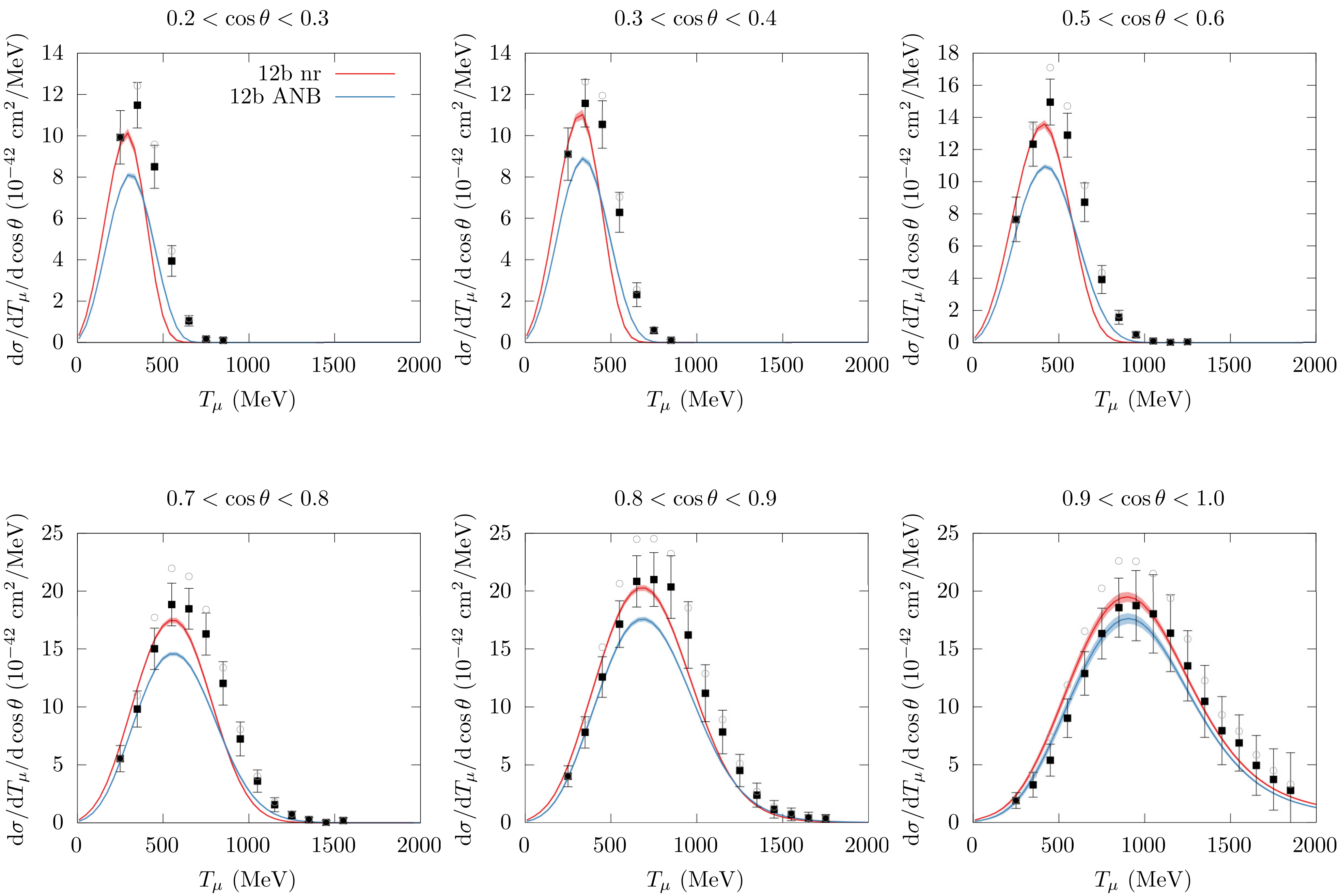

Noemi Rocco, nrocco@fnal.gov

Cross sections: Green's Function Monte Carlo

Electron scattering results including relativistic corrections for some kinematics covered by the calculated responses

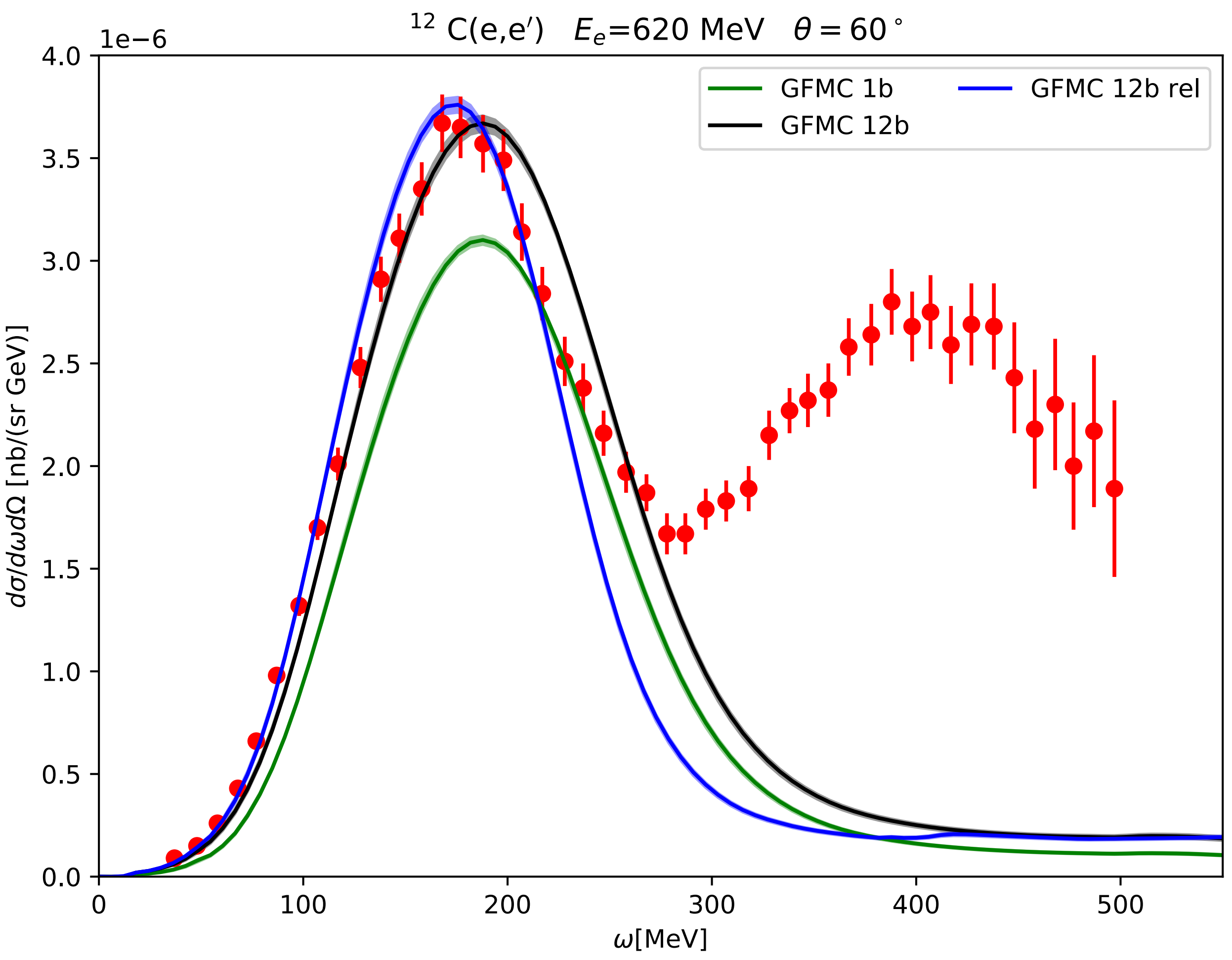

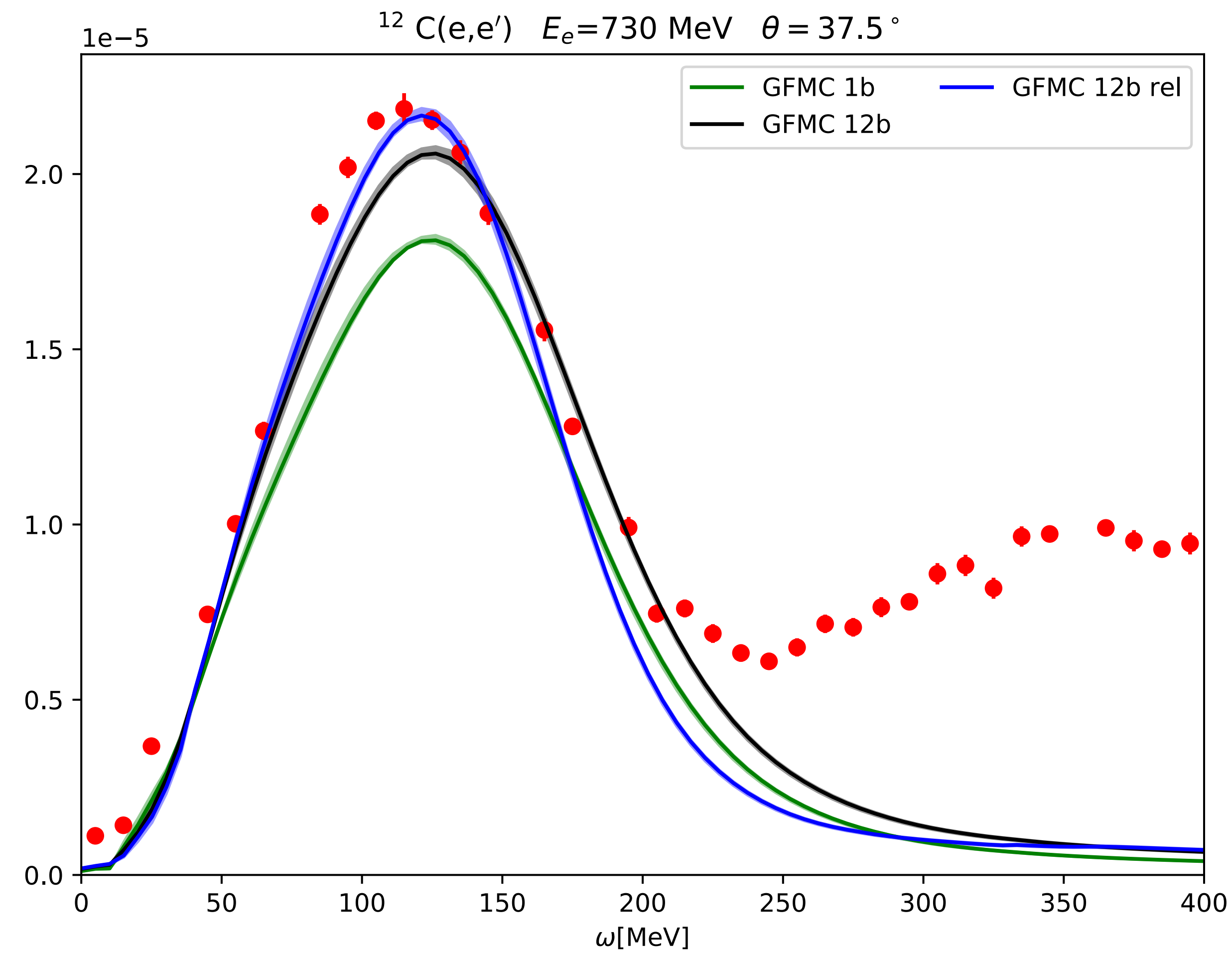

A.Lovato, A.Nikolakopoulos, NR, N. Steinberg, Universe 9 (2023) 8, 36

Address new experimental capabilities

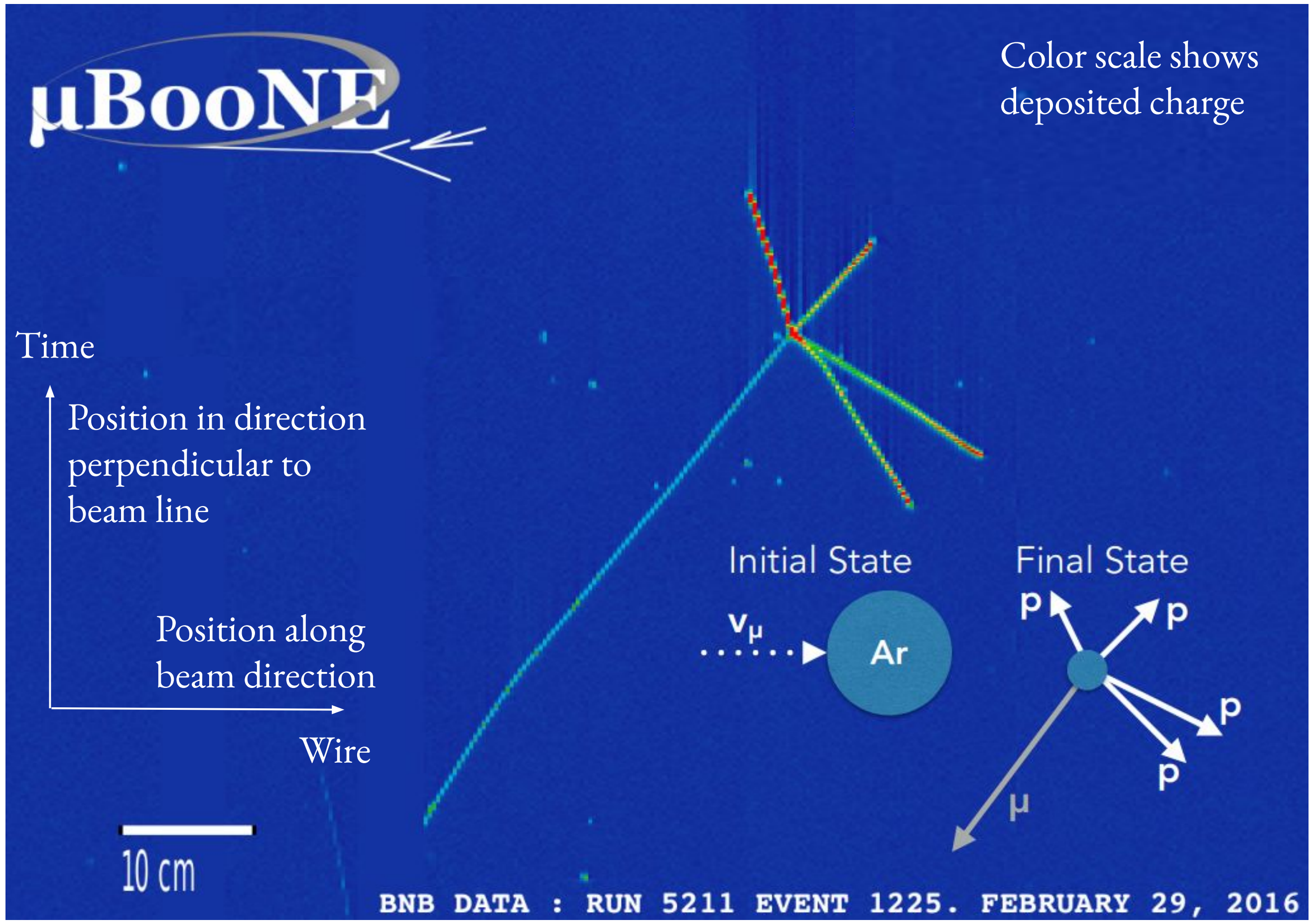

T.Sato talks @ NuSTEC Workshop on Neutrino-Nucleus Pion Production in the Resonance Region

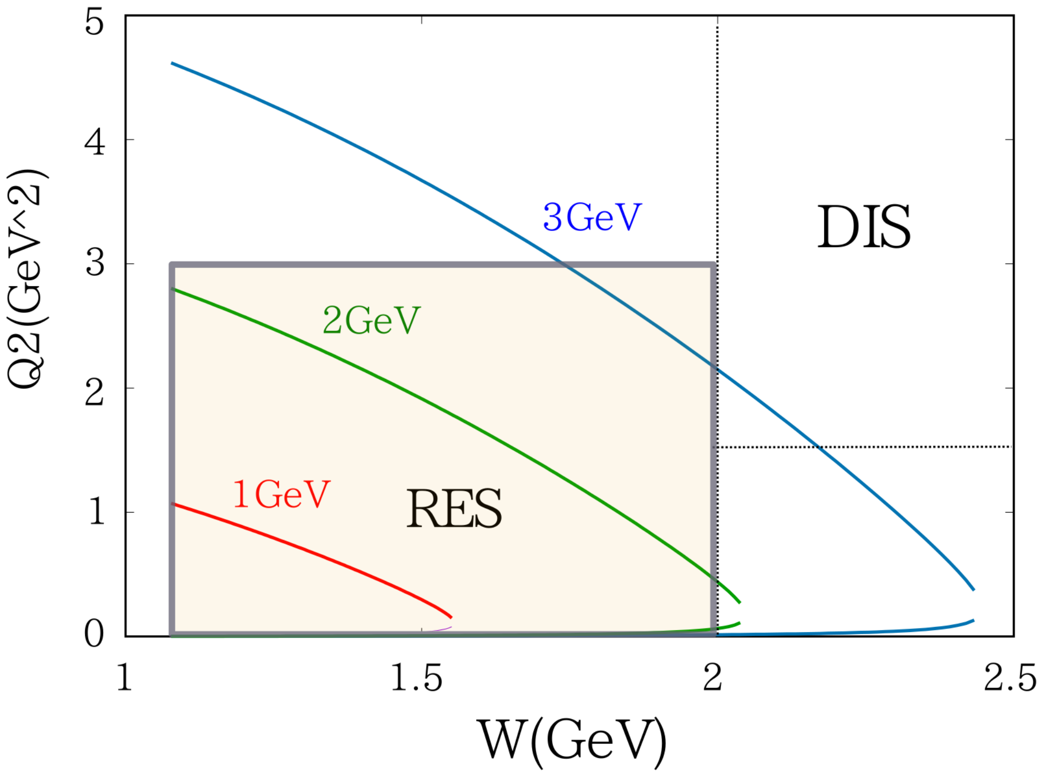

- Excellent spatial resolution
- Precise calorimetric information
- Powerful particle identification

$$W = \sqrt{(p+q)^2}, Q^2 = -q^2 = -(p_\nu - p_l)^2$$

Noemi Rocco, nrocco@fnal.gov

Factorization Based Approaches

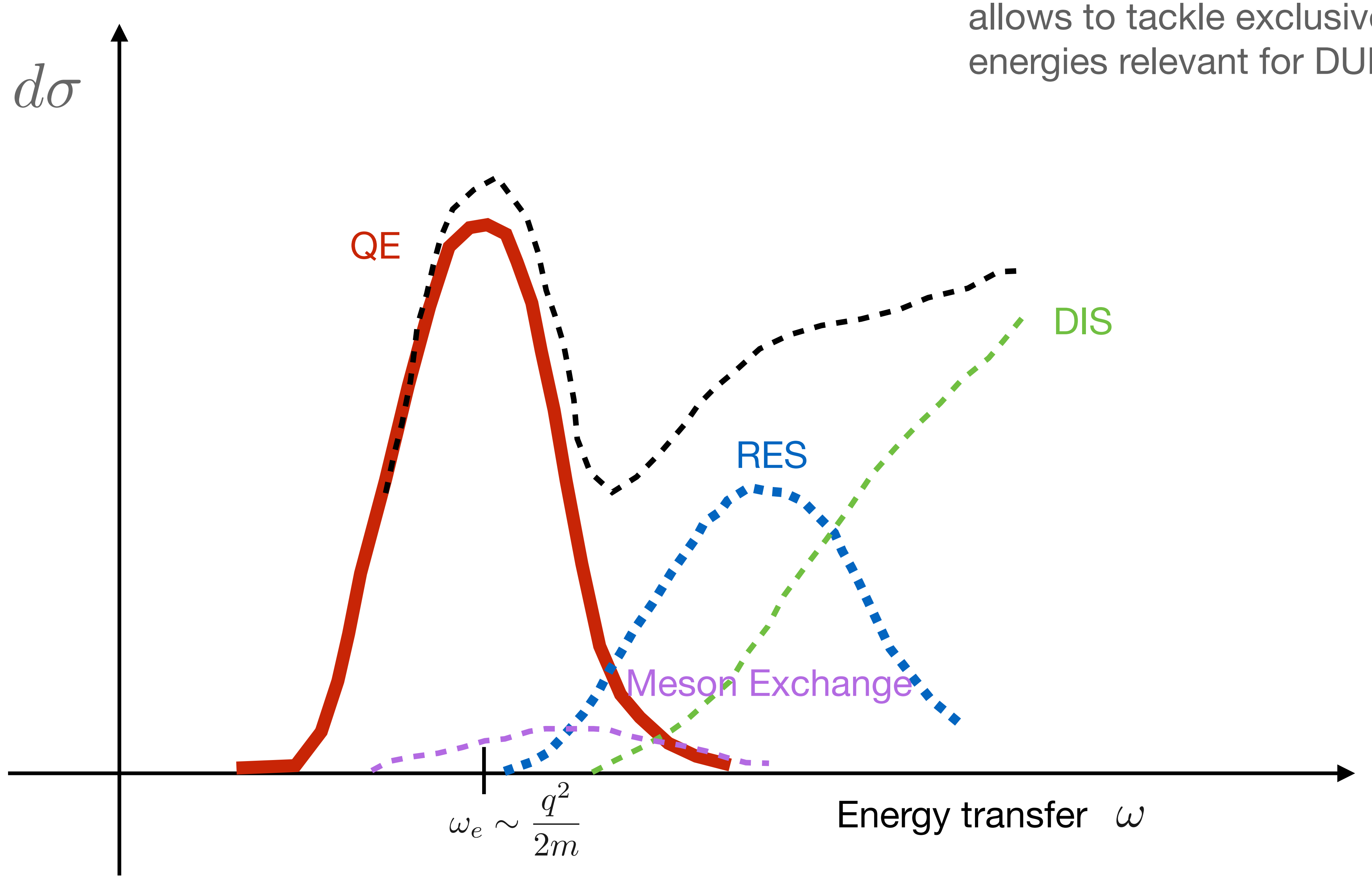

Factorization of the hadronic final states: allows to tackle exclusive channels + higher energies relevant for DUNE

Noemi Rocco, nrocco@fnal.gov

Spectral function approach

At large momentum transfer, the scattering reduces to the sum of individual terms

$$J_\alpha = \sum_i j^i_\alpha \qquad\qquad |\Psi_f\rangle \to |p\rangle \otimes |\Psi_f\rangle_{A-1}$$

The incoherent contribution of the one-body response reads

$$R_{\alpha\beta} \simeq \int \frac{d^3k}{(2\pi)^3} dE P_h(\mathbf{k}, E) \sum_i \langle k | {j^i_\alpha}^\dagger | k+q\rangle \langle k+q | j^i_\beta | k\rangle \delta(\omega + E - e(\mathbf{k}+\mathbf{q}))$$

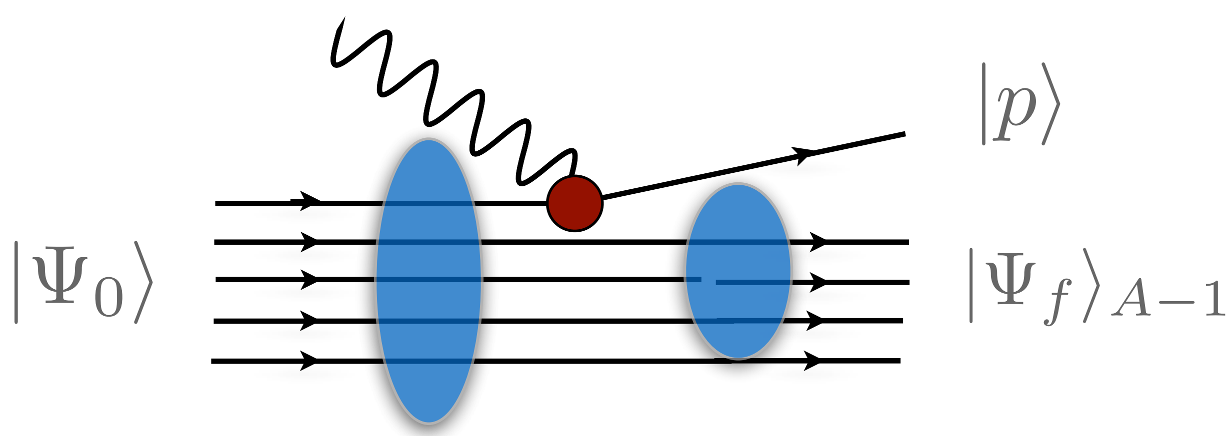

The Spectral Function is the imaginary part of the two point Green's Function

Different many-body methods can be adopted to determine it

O. Benhar et al, Rev.Mod.Phys. 80 (2008)

I. Korover, et al Phys.Rev.C 107 (2023) 6, L061301

***NR,* Frontiers in Phys. 8 (2020) 116**

J.E. Sobczyk et al, PRC 106 (2022) 3

J.E. Sobczyk et al, PRC 109 (2024)

QMC Spectral function of light nuclei

- Single-nucleon spectral function:

$$P_{p,n}(\mathbf{k},E) = \sum_n \left| \langle \Psi_0^A | [|k\rangle \otimes |\Psi_n^{A-1}\rangle] \right|^2 \delta(E + E_0^A - E_n^{A-1}) = P^{MF}(\mathbf{k},E) + P^{\rm corr}(\mathbf{k},E)$$

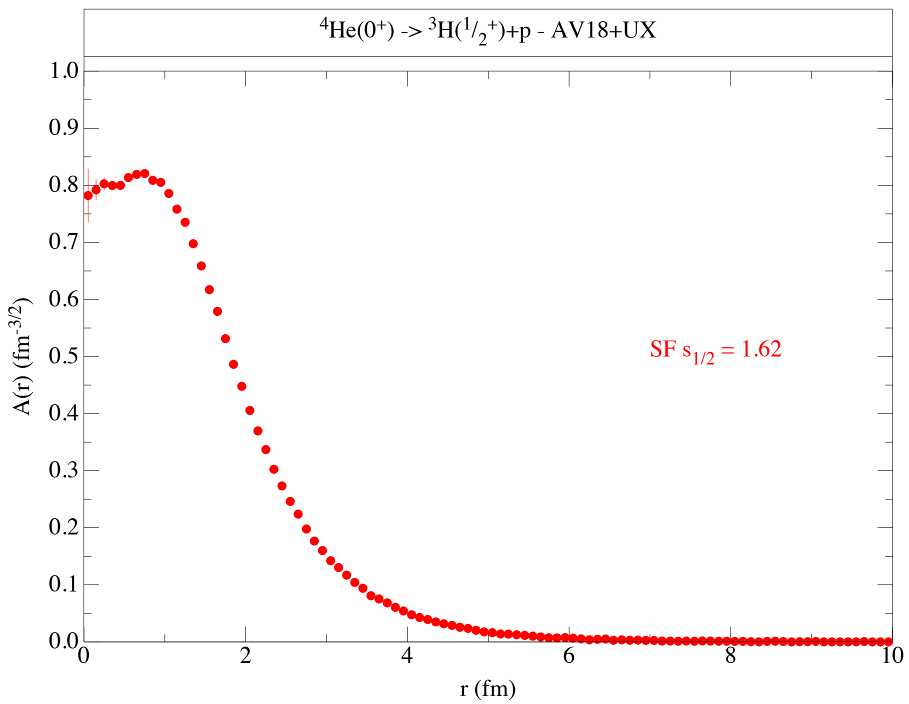

$$P^{MF}(\mathbf{k},E) = \left| \langle \Psi_0^A | [|k\rangle \otimes |\Psi_n^{A-1}\rangle] \right|^2 \times \delta\left(E - B_A + B_{A-1} - \frac{\mathbf{k}^2}{2m_{A-1}}\right)$$

- The single-nucleon overlap has been computed within VMC (center of mass motion fully accounted for)

$$P^{\rm corr}(\mathbf{k},E) = \int d^3k' \left| \langle \Psi_0^A | [|k\rangle |k'\rangle \otimes |\Psi_n^{A-2}\rangle] \right|^2 \times \delta\left(E - B_A - e(\mathbf{k}') + B_{A-2} - \frac{(\mathbf{k}+\mathbf{k}')^2}{2m_{A-2}}\right)$$

- Written in terms of two-body momentum distribution

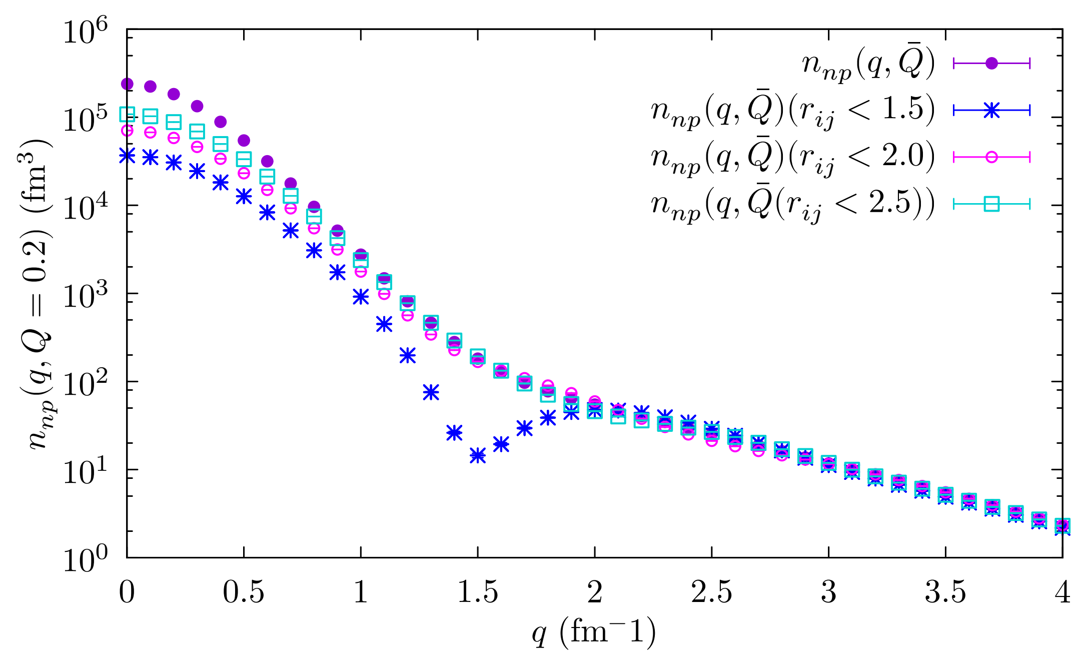

Noemi Rocco, nrocco@fnal.gov

Spectral function approach

$$\boxed{|f\rangle \to |pp'\rangle_a \otimes |f_{A-2}\rangle}$$

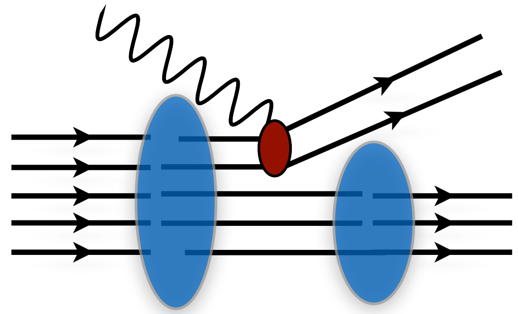

The hadronic tensor for two-body current factorizes as

$$R^{\mu\nu}_{2\mathrm{b}}(\mathbf{q},\omega) \propto \int dE d^3k d^3k' P_{2\mathrm{b}}(\mathbf{k},\mathbf{k}',E) \times d^3p d^3p' |\langle kk'|j^\mu_{2\mathrm{b}}|pp'\rangle|^2$$

$$\boxed{|f\rangle \to |p_\pi p\rangle \otimes |f_{A-1}\rangle}$$

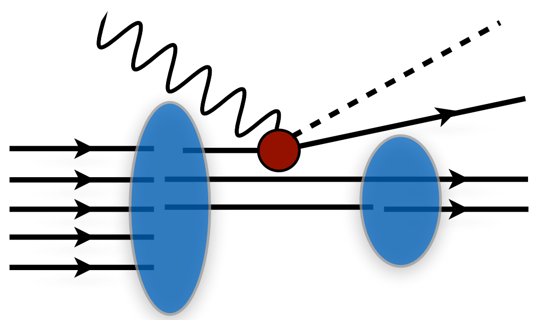

Production of real π in the final state

$$R^{\mu\nu}_{1\mathrm{b}\pi}(\mathbf{q},\omega) \propto \int dE d^3k P_{1\mathrm{b}}(\mathbf{k},E) \times d^3p d^3k_\pi |\langle k|j^\mu|pk_\pi\rangle|^2$$

- Pion production elementary amplitudes currently derived within the extremely sophisticated **Dynamic Couple Chanel approach**;

S.X.Nakamura, et al PRD92(2015)
T. Sato, et al PRC67(2003)

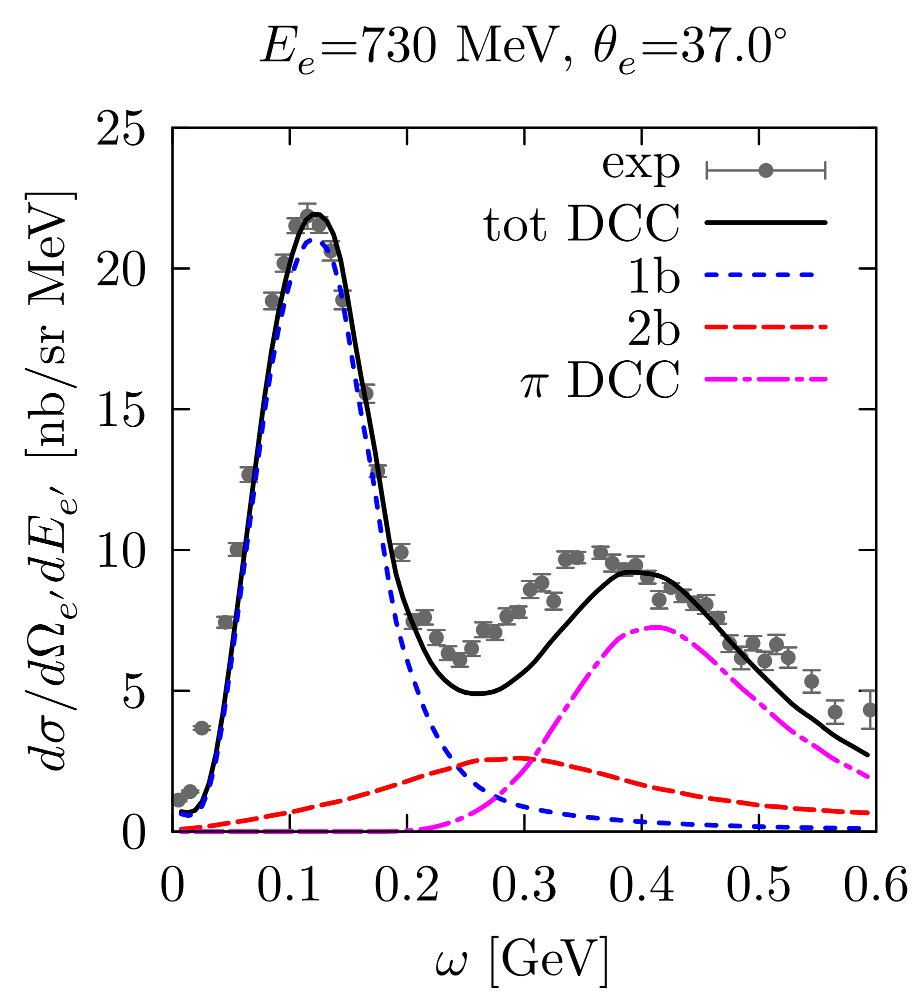

***NR*, Frontiers in Phys. 8 (2020) 116**

Axial Form Factors Uncertainty needs

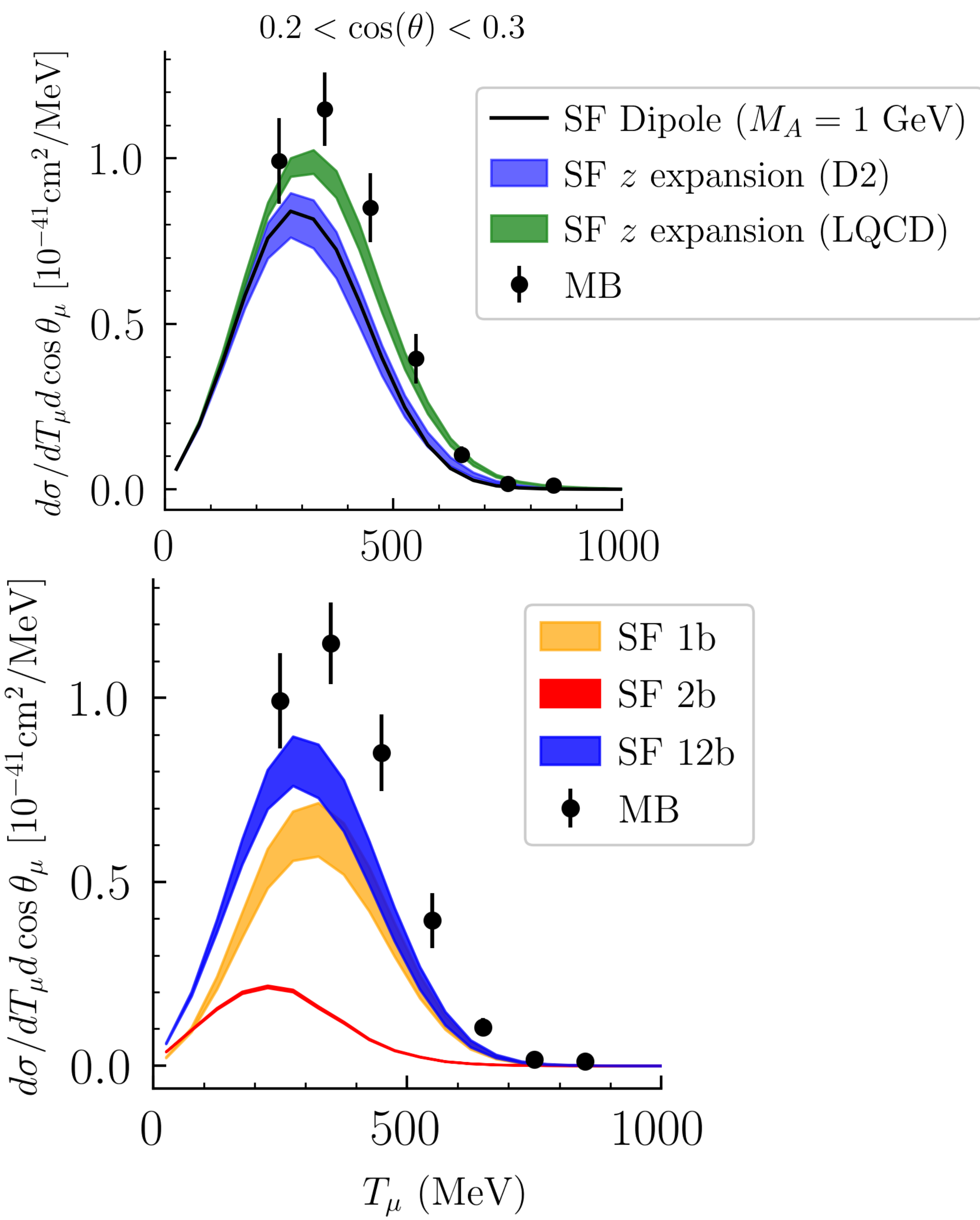

D.Simons, N. Steinberg et al, 2210.02455

✴ Axial form factor dependence:

MiniBooNE	$0.2 < \cos\theta_\mu < 0.3$
SF Difference in $d\sigma_{\mathrm{peak}}$ (%)	16.3

✴ Many-body method dependence:

MiniBooNE	$0.2 < \cos\theta_\mu < 0.3$
GFMC/SF difference in $d\sigma_{\mathrm{peak}}$ (%)	22.8

Noemi Rocco, nrocco@fnal.gov

Axial Form Factors Uncertainty needs

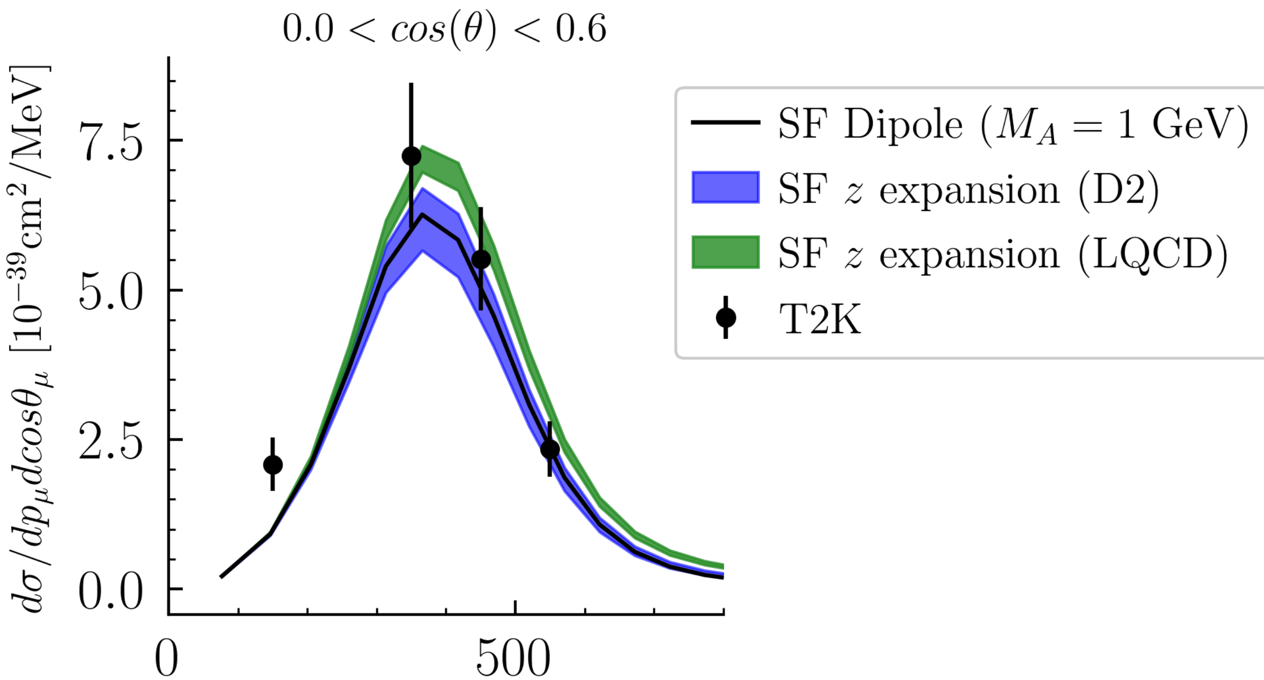

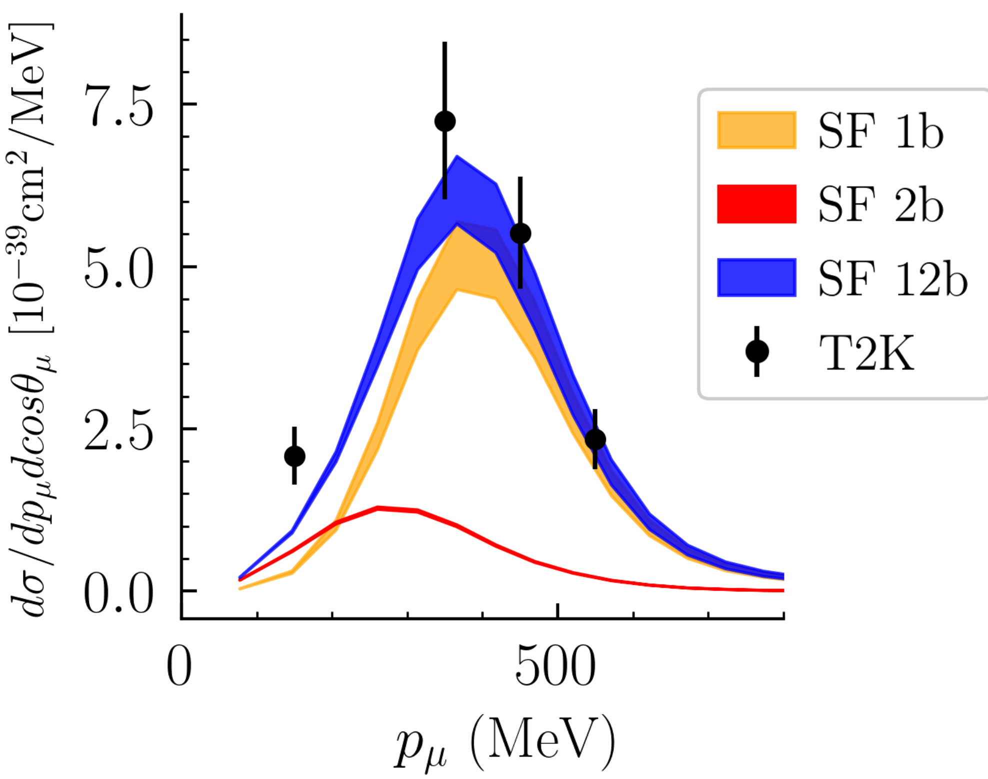

D.Simons, N. Steinberg et al, 2210.02455

✳ Axial form factor dependence:

T2K	$0.0 < \cos\theta_\mu < 0.6$
SF difference in $d\sigma_{\text{peak}}$ (%)	15.3

✳ Many-body method dependence:

T2K	$0.0 < \cos\theta_\mu < 0.6$
GFMC/SF difference in $d\sigma_{\text{peak}}$ (%)	13.4

Noemi Rocco, nrocco@fnal.gov

Two-body currents - Delta contribution

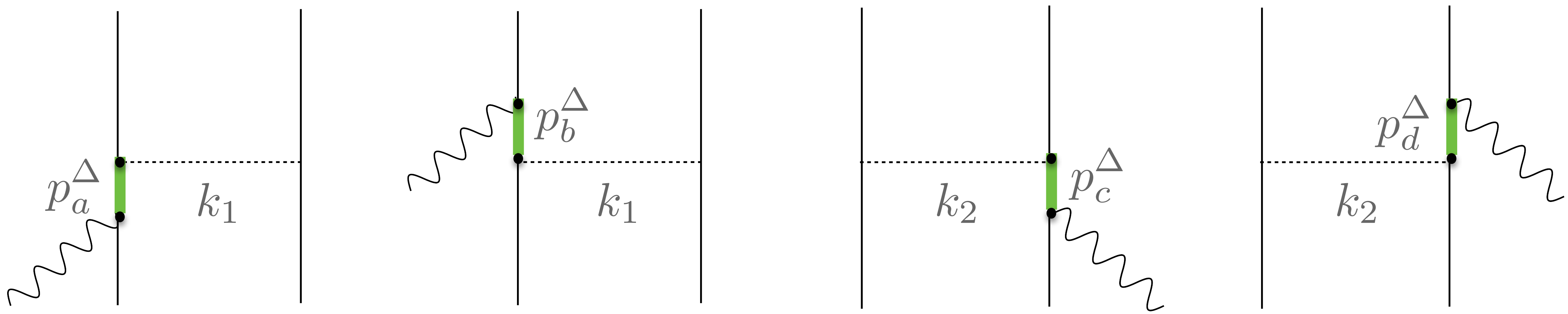

$$j^\mu_\Delta = \frac{3}{2}\frac{f_{\pi NN} f^*}{m_\pi^2}\Big\{\Pi(k_2)_{(2)}\Big[\Big(-\frac{2}{3}\tau^{(2)} + \frac{I_V}{3}\Big)_z F_{\pi NN}(k_2) F_{\pi N\Delta}(k_2)(J^\mu_a)_{(1)}$$
$$-\Big(\frac{2}{3}\tau^{(2)} + \frac{I_V}{3}\Big)_z F_{\pi NN}(k_2) F_{\pi N\Delta}(k_2)(J^\mu_b)_{(1)}\Big] + (1 \leftrightarrow 2)\Big\}$$

where

Rarita Schwinger propagator

$$(j^\mu_a)_V = (k'_\pi)^\alpha G_{\alpha\beta}(p_\Delta)\Big[\frac{C_3^V}{m_N}(g^{\beta\mu}\not{q} - q^\beta\gamma^\mu)\gamma_5\Big] \qquad (j^\mu_a)_A = (k'_\pi)^\alpha G_{\alpha\beta}(p_\Delta) C_5^A g^{\beta\mu}$$

Noemi Rocco, nrocco@fnal.gov

Resonance Uncertainty needs

The largest contributions to two-body currents arise from resonant $N \to \Delta$ transitions yielding pion production

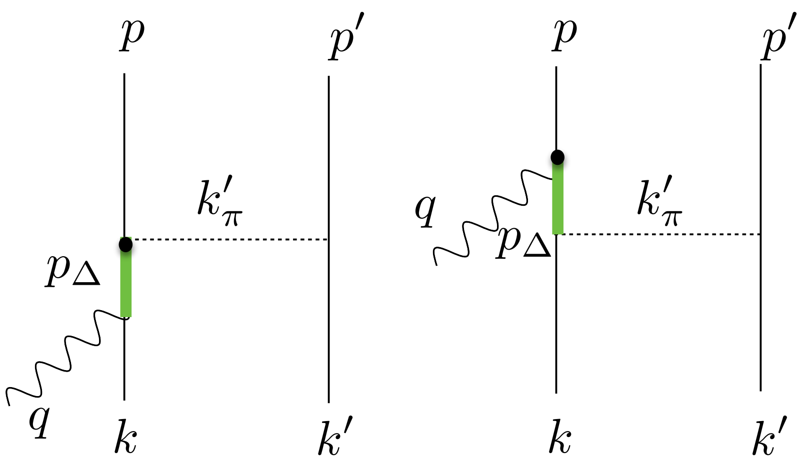

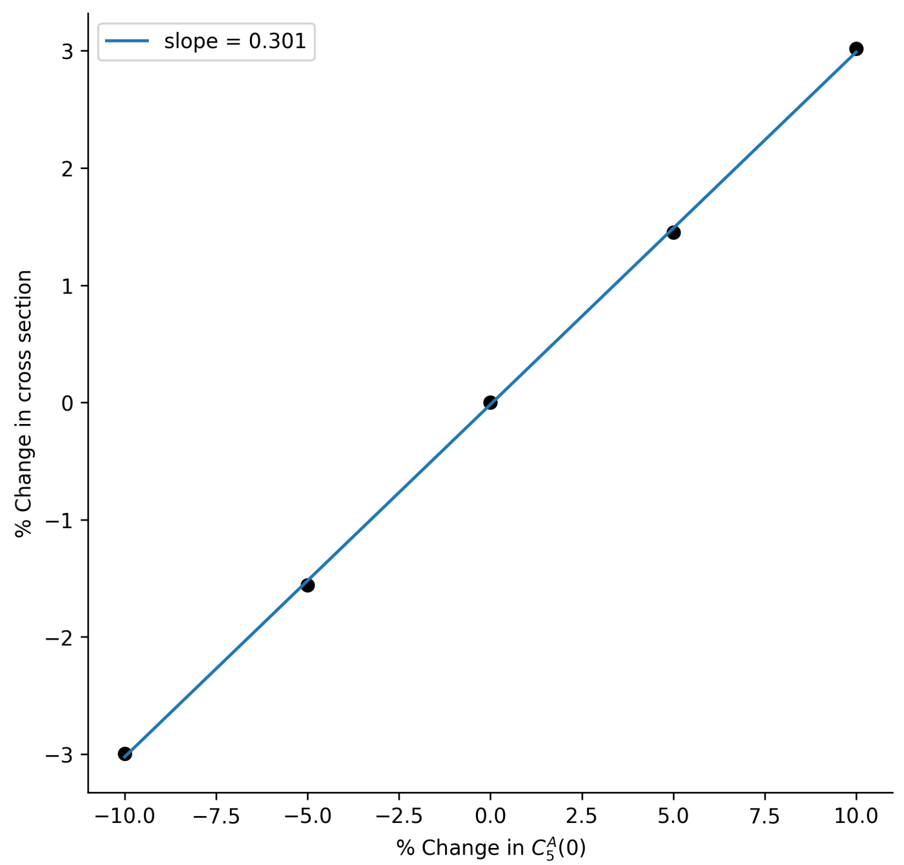

The normalization of the dominant $N \to \Delta$ transition form factor needs be known to 3% precision to achieve 1% cross-section precision for MiniBooNE kinematics

D.Simons, N. Steinberg et al, 2210.02455

State-of-the-art determinations of this form factor from experimental data on pion electroproduction achieve 10-15% precision (under some assumptions)

Hernandez et al, PRD 81 (2010)

Further constraints on $N \to \Delta$ transition relevant for two-body currents and π production will be necessary to achieve few-percent cross-section precision

Including the one- and two-body interference

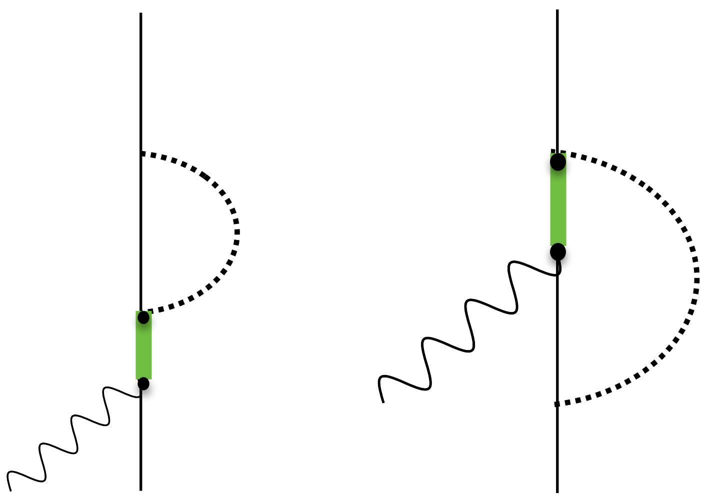

We recently included interference effects between one- and two-body currents yielding single nucleon knock-out

Observe a small quenching in the longitudinal channel and an enhancement in the q.e. peak in the transverse → agreement with the GFMC

N. Steinberg, NR, A. Lovato, arXiv: 2312.12545

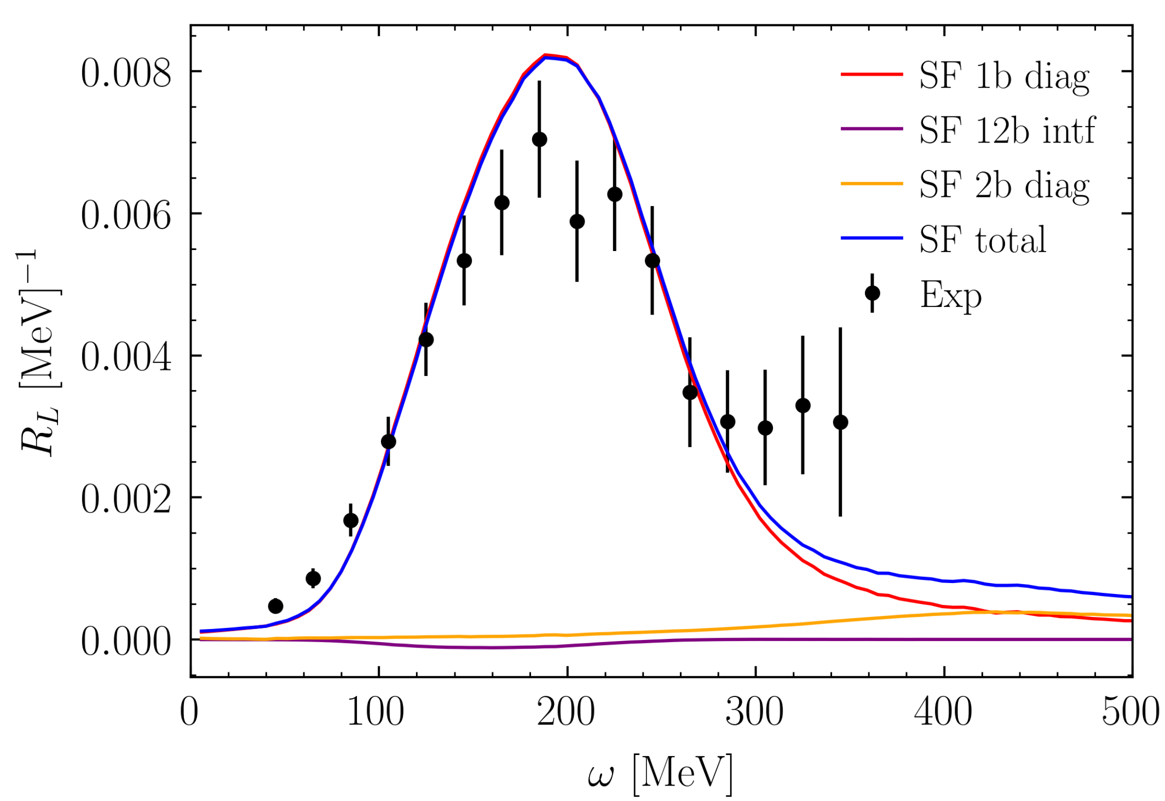

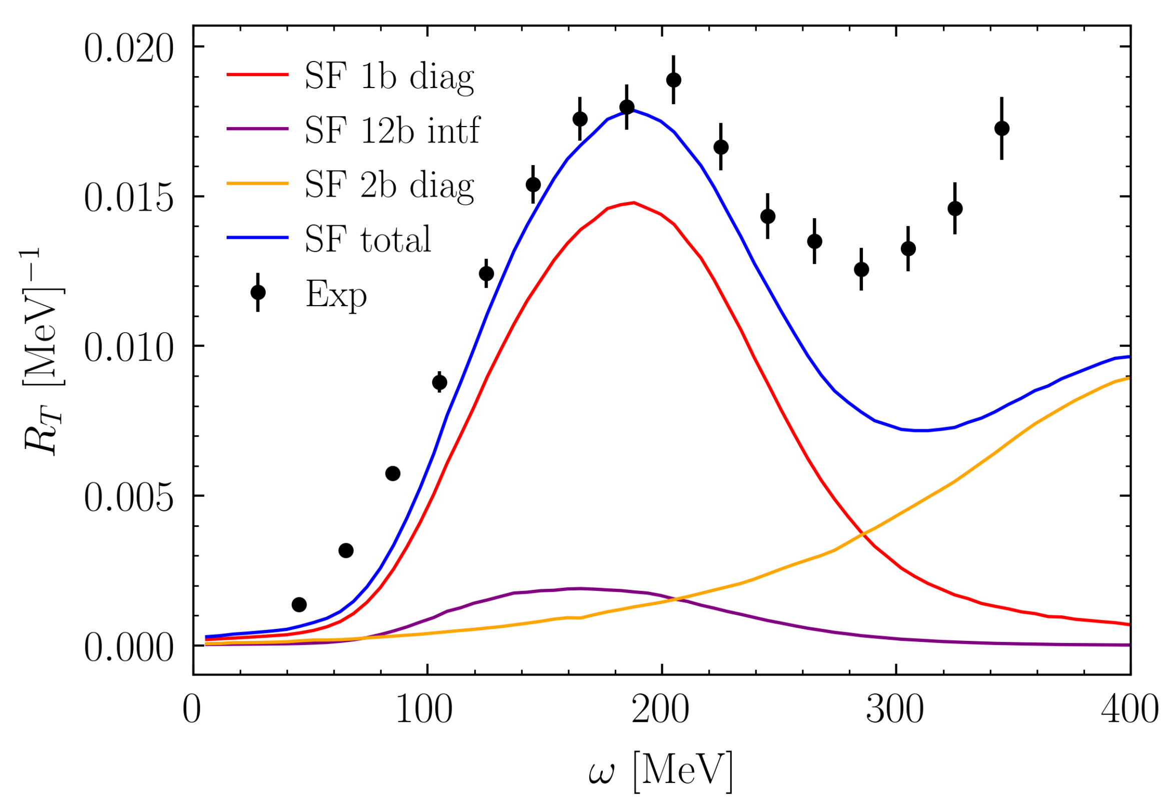

Fermilab

Noemi Rocco, nrocco@fnal.gov

Including the one- and two-body interference

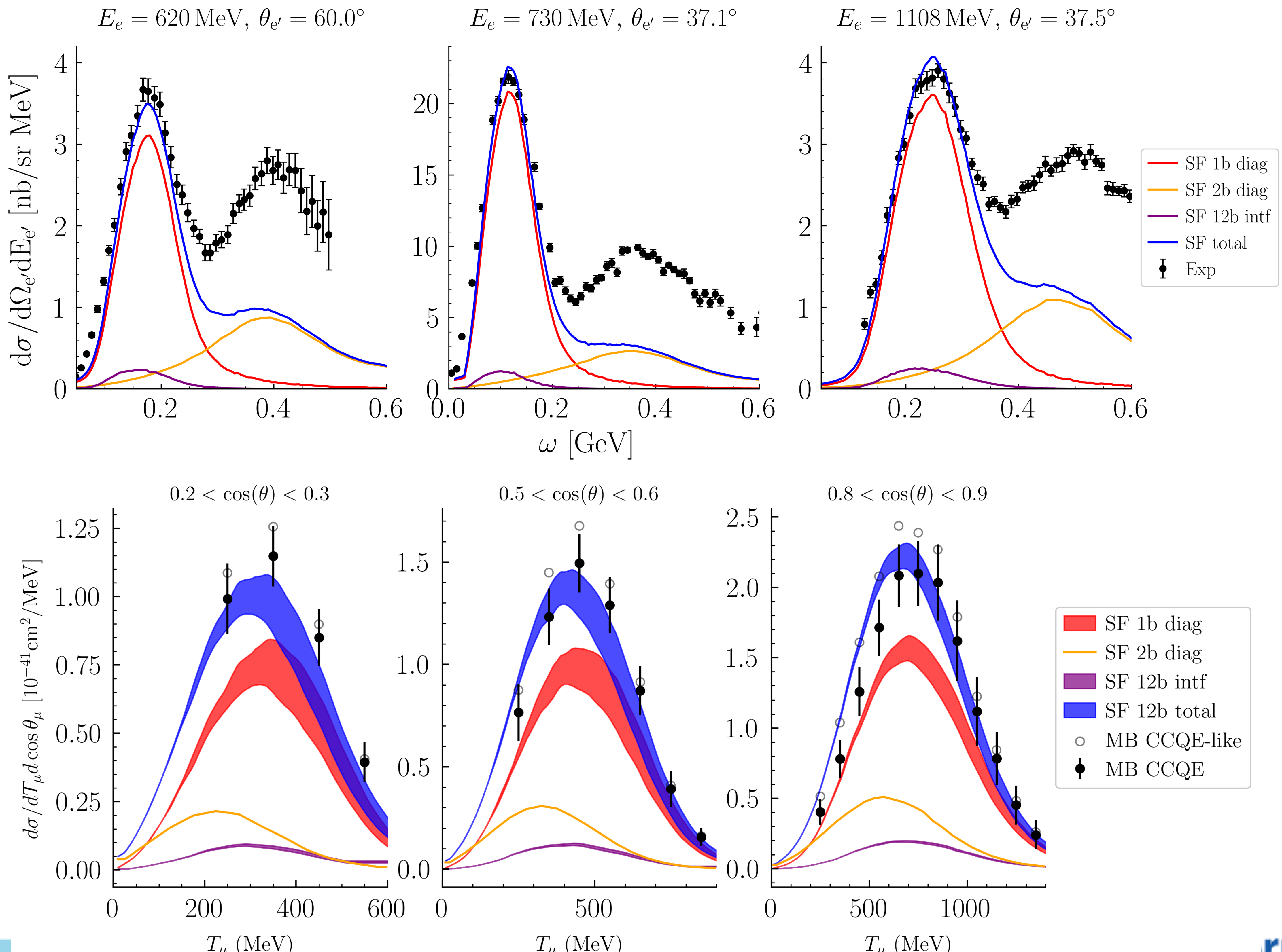

N. Steinberg, NR, A. Lovato, arXiv: 2312.12545

Interplay with BSM scenarios

Z. Tabrizi, J. Kopp, NR, arxiv: 2401.07902

- Interested in Weak Effective Field Theory (WEFT), valid below the electroweak scale, with the electroweak gauge bosons, the Higgs boson, and the top quark integrated out

- CC: New left/right handed, (pseudo)scalar and tensor interactions

$$
\begin{aligned}
\mathcal{L}_{\mathrm{WEFT}} \supset \; & -\frac{2V_{ud}}{v^2}\Big\{ [\mathbf{1} + \epsilon_L]_{\alpha\beta} (\bar{u}\gamma^\mu P_L d)(\bar{\ell}_\alpha \gamma_\mu P_L \nu_\beta) \\
& + [\epsilon_R]_{\alpha\beta} (\bar{u}\gamma^\mu P_R d)(\bar{\ell}_\alpha \gamma_\mu P_L \nu_\beta) \\
& + \frac{1}{2}[\epsilon_S]_{\alpha\beta} (\bar{u} d)(\bar{\ell}_\alpha P_L \nu_\beta) - \frac{1}{2}[\epsilon_P]_{\alpha\beta} (\bar{u}\gamma_5 d)(\bar{\ell}_\alpha P_L \nu_\beta) \\
& + \frac{1}{4}[\hat{\epsilon}_T]_{\alpha\beta} (\bar{u}\sigma^{\mu\nu} P_L d)(\bar{\ell}_\alpha \sigma_{\mu\nu} P_L \nu_\beta) + \mathrm{h.c.}\Big\}
\end{aligned}
$$

- SM Interactions:

V : $$\langle p(p_p)|\bar{q}_u\gamma_\mu q_d|n(p_n)\rangle = \bar{u}_p(p_p)\left[G_V(Q^2)\gamma_\mu + i\frac{\tilde{G}_{T(V)}(Q^2)}{2M_N}\sigma_{\mu\nu}q^\nu - \cancel{\frac{\tilde{G}_S(Q^2)}{2M_N}q_\mu}\right]u_n(p_n)$$

A : $$\langle p(p_p)|\bar{q}_u\gamma_\mu\gamma_5 q_d|n(p_n)\rangle = \bar{u}_p(p_p)\left[G_A(Q^2)\gamma_\mu\gamma_5 + i\cancel{\frac{\tilde{G}_{T(A)}(Q^2)}{2M_N}}\sigma_{\mu\nu}q^\nu\gamma_5 - \frac{\tilde{G}_P(Q^2)}{2M_N}q_\mu\gamma_5\right]u_n(p_n)$$

Form factors - new interactions

Z. Tabrizi, J. Kopp, NR, arxiv: 2401.07902

- Scalar: conservation of the vector current (CVC)

$$G_S(Q^2) = -\frac{\delta M_N^{QCD}}{\delta m_q} G_V(Q^2) + \frac{Q^2/2M_N}{\delta m_q}\tilde{G}_S(Q^2)$$

small

- Partially-conserved axial current (PCAC)

$$G_P(Q^2) = \frac{M_N}{m_q} G_A(Q^2) + \frac{Q^2/2M_N}{2m_q}\tilde{G}_P(Q^2)$$

- Tensor: LQCD and theoretical considerations

We can not neglect $\tilde{G}_S(Q^2)$ anymore.

We analyze for the first time how the **axial form factor uncertainty affects the study of new interactions** beyond the SM and we find a sizable effect

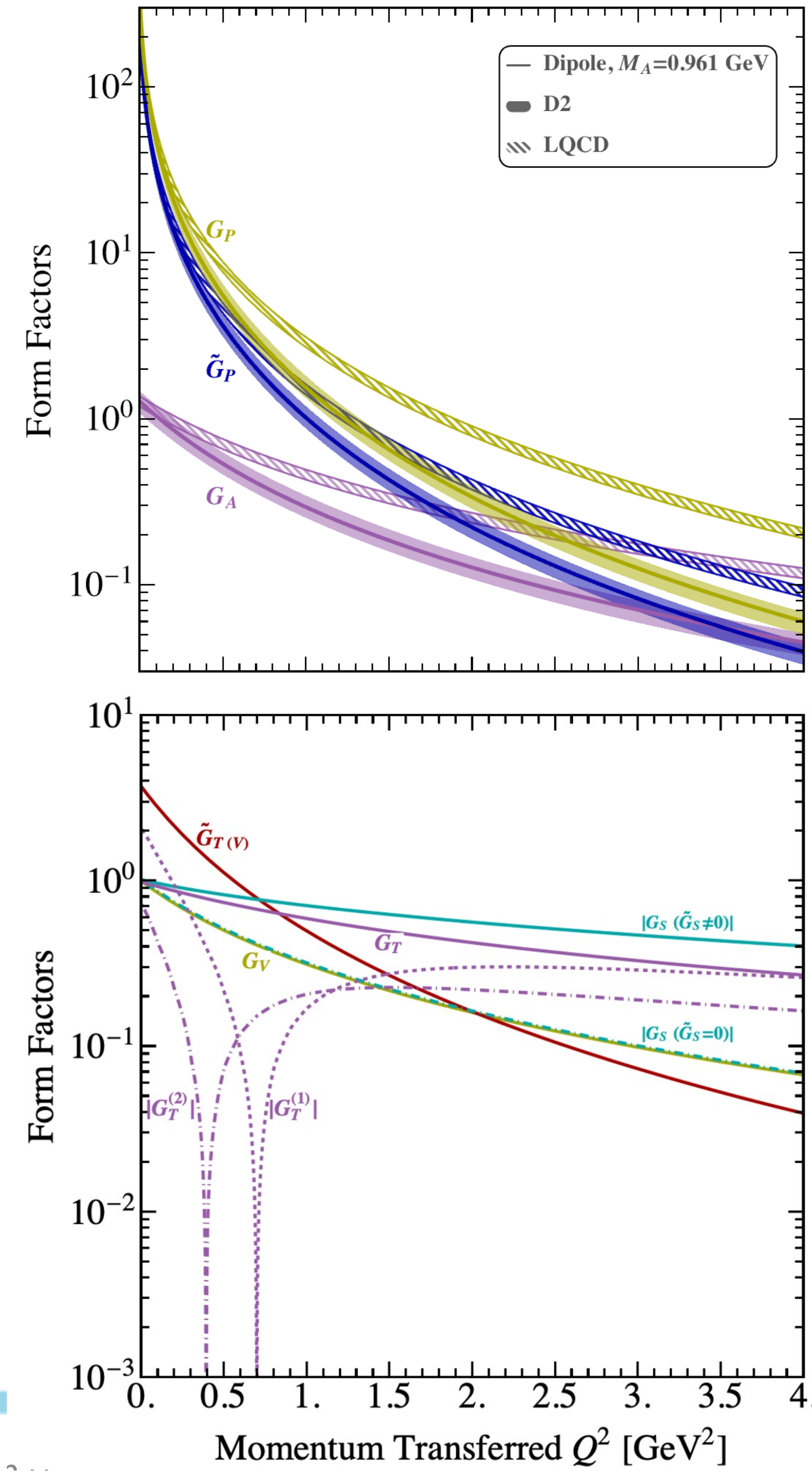

Interplay with BSM scenarios

Z. Tabrizi, J. Kopp, NR, arxiv: 2401.07902

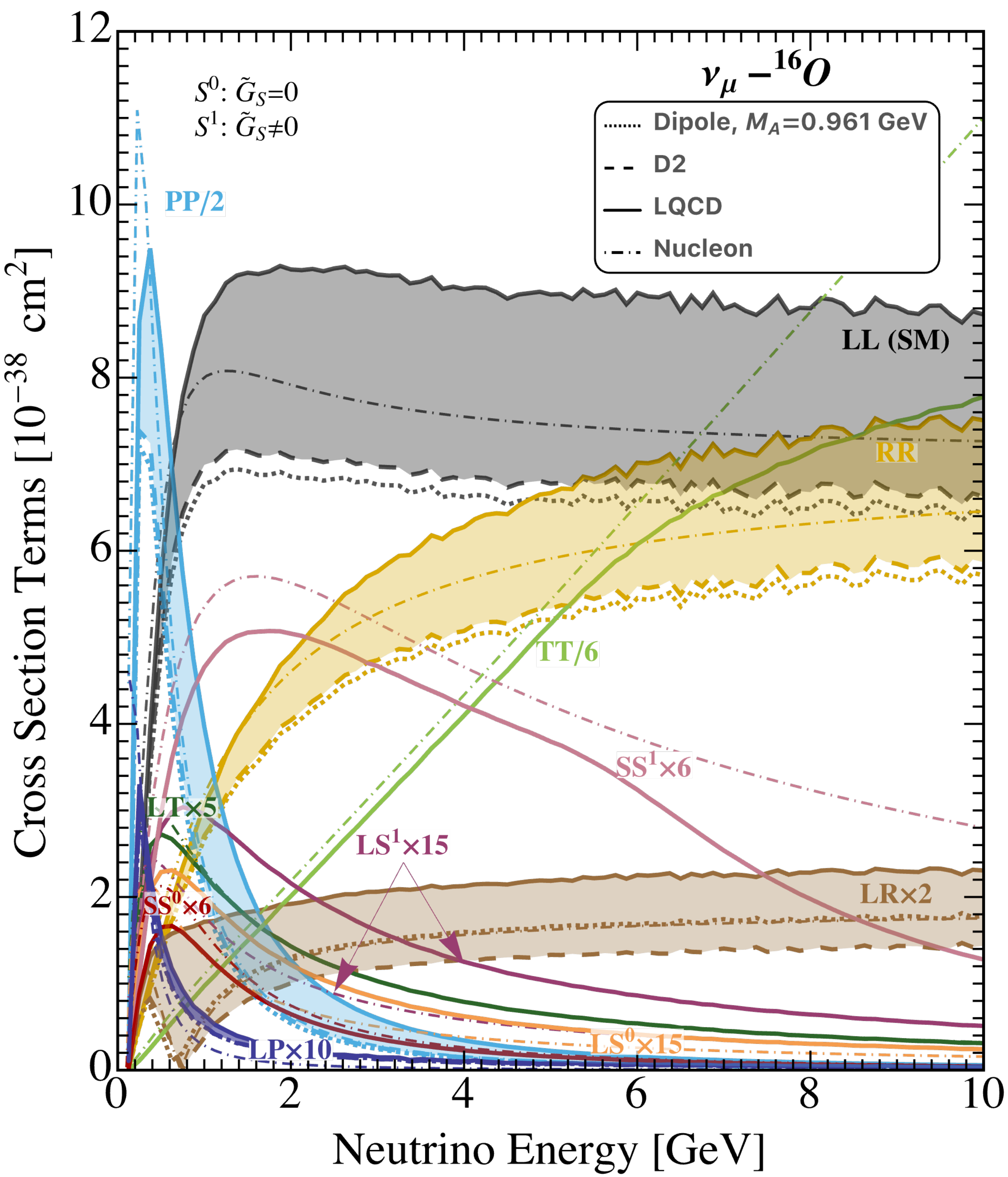

- Specific Lorentz structures, especially pseudoscalar and tensor interactions, exhibit cross sections notably enhanced compared to those of the Standard Model. {there is a considerable margin of uncertainty}
- The axial form factor introduces significant systematic uncertainties, true for both SM and BSM interactions
- Nuclear effects are crucial even at multi-GeV energies, this is particularly apparent for tensor interactions at energies ≳ 6GeV

Using Bayesian ANN for electron-nucleus scattering

J. Sobczyk, NR, A. Lovato, arxiv:2406.06292

The inclusive electron-nucleus cross section can be written in terms of the longitudinal and transverse response function

$$\left(\frac{d^2\sigma}{dE'd\Omega'}\right)_e = \left(\frac{d\sigma}{d\Omega'}\right)_{\rm M}\left[\frac{q^4}{\mathbf{q}^4}R_L(\mathbf{q},\omega) + \left(\tan^2\frac{\theta}{2} - \frac{1}{2}\frac{q^2}{\mathbf{q}^2}\right)R_T(\mathbf{q},\omega)\right]$$

Traditionally, the **Rosenbluth separation** is adopted to obtain $R_L(\mathbf{q},\omega)$ and $R_T(\mathbf{q},\omega)$

$$\Sigma(\mathbf{q},\omega,\epsilon) = \epsilon\,\frac{\mathbf{q}^4}{Q^4}\left(\frac{d^2\sigma}{dE'd\Omega'}\right)_e \Bigg/ \left(\frac{d\sigma}{d\Omega'}\right)_{\rm M} = \epsilon R_L(\mathbf{q},\omega) + \frac{1}{2}\frac{\mathbf{q}^2}{Q^2}R_T(\mathbf{q},\omega)$$

Photon polarization

As θ ranges between 180 to 0 degrees, ϵ varies between 0 and 1. Within this approach, R_L is the **slope** while $(\mathbf{q}^2/2Q^2)R_T$ is the **intercept** of the linear fit to data

This definition can only be applied if the Born approximation is valid and if the data have already been corrected to account for Coulomb distortions of the electron wave function.

Using Bayesian ANN for electron-nucleus scattering

We used ANN architecture to obtain the **longitudinal** and **transverse responses**

- We preprocess the input through a ‘scaling’ net whose output is $y(\mathbf{q}, \omega, A, Z)$.
- We concatenate y with the other inputs to compute the ‘Response’ net which gives a 32-dim output.
- This input is used to built **two completely independent nets**; each provides a single output corresponding to the longitudinal and transverse responses, respectively.

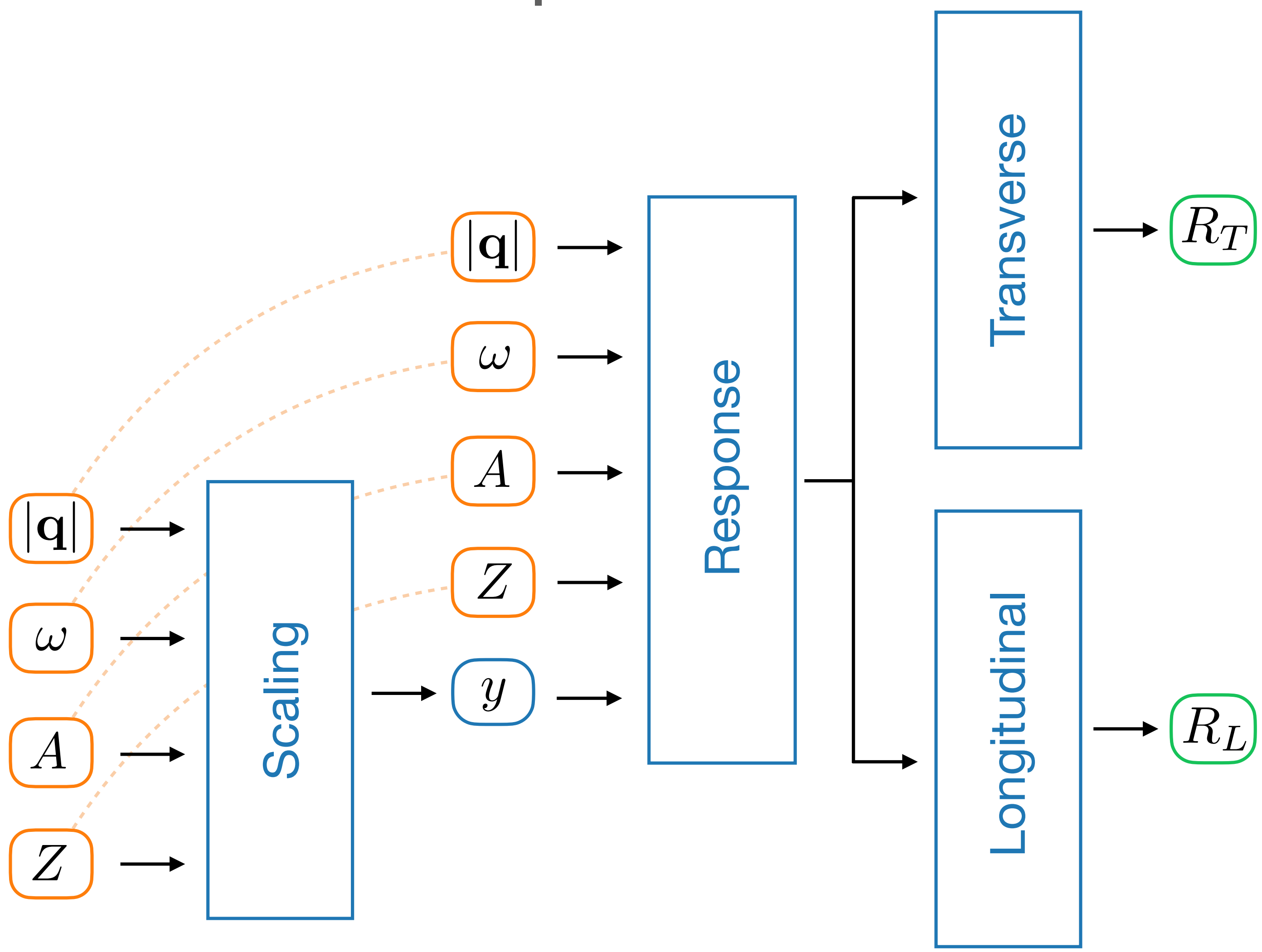

We train our ANN using the quasielastic electron nucleus scattering archive of arXiv:nucl-ex/0603032 considering five different light and medium-mass nuclei, symmetric: ^{4}He, ^{6}Li, ^{12}C, ^{16}O and ^{40}Ca.

Noemi Rocco, nrocco@fnal.gov

Using Bayesian ANN for electron-nucleus scattering

We used **Bayesian statistics** to quantify the uncertainty of the ANN. We treat the weights $\mathscr{W}$ as a probability distribution.

The posterior probability of the parameters $\mathscr{W}$ given the measured cross sections Y can be written as

$$P(\mathscr{W}\,|\,Y) = \frac{P(Y\,|\,\mathscr{W})P(\mathscr{W})}{P(Y)}$$

We assign a normal Gaussian prior for each neural network parameter and assume a **Gaussian distribution for the likelihood** based on a loss function obtained from a **least-squares** fit to the empirical data

$$P(Y\,|\,\mathscr{W}) = \exp\left(-\frac{\chi^2}{2}\right) \qquad \chi^2 = \sum_{i=1}^{N} \frac{\left[y_i - \hat{y}_i(\mathscr{W})\right]^2}{\sigma_i^2}$$

We increase the experimental errors σ_i listed in arXiv:nucl-ex/0603032 including an additional term proportional to the experimental cross section value: $\sigma_i \rightarrow \sigma_i + 0.05 y_i$.

The posterior distribution is sampled using the **NumPyro No-U-Turn Sampler** extension of HMC. We also implemented the standard HMC algorithm and validated results.

Noemi Rocco, nrocco@fnal.gov

Using Bayesian ANN for electron-nucleus scattering

J. Sobczyk, NR, A. Lovato, arxiv:2406.06292

Results: Cross sections for different nuclei

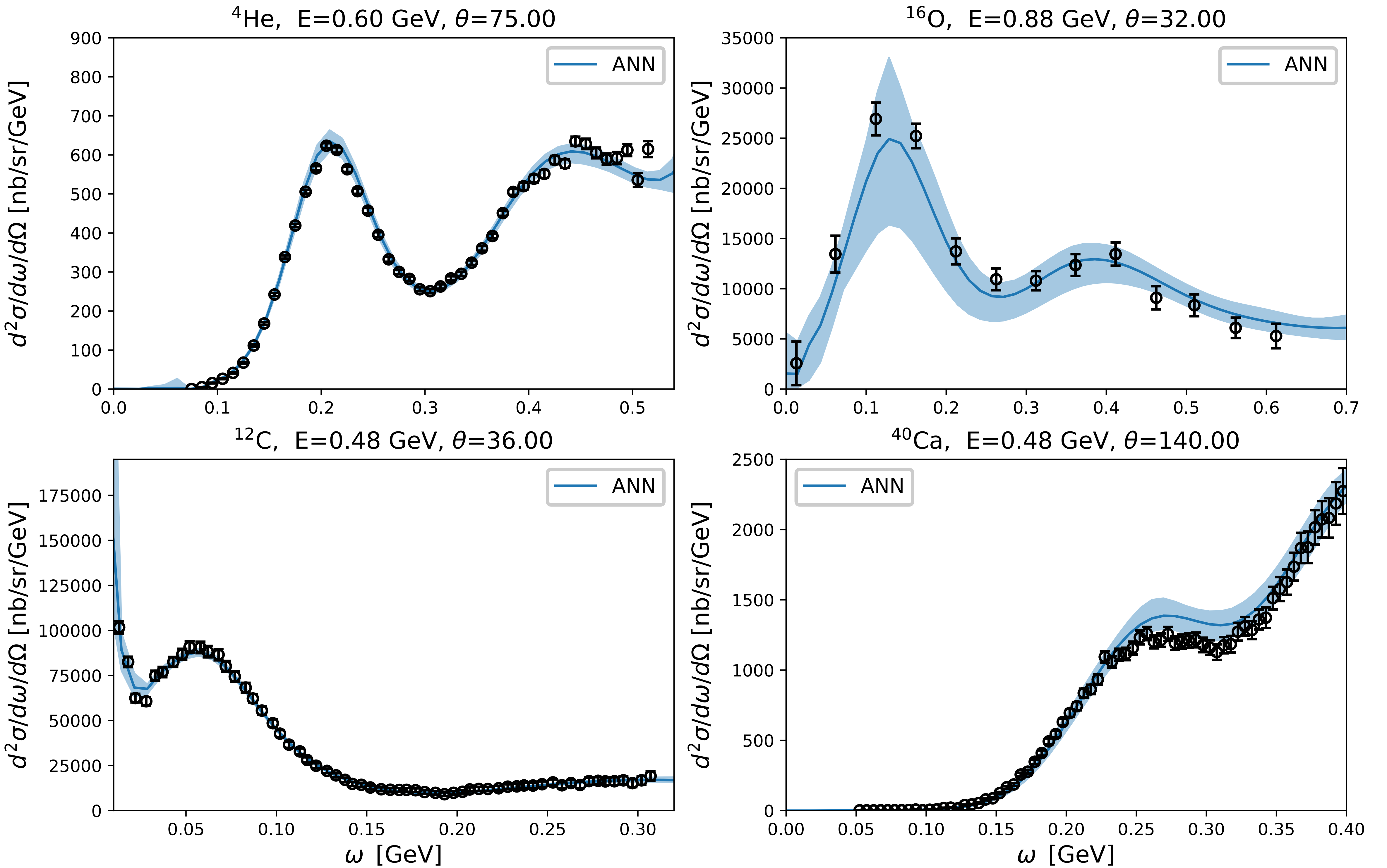

Using Bayesian ANN for electron-nucleus scattering

J. Sobczyk, NR, A. Lovato, arxiv:2406.06292

Results: Electromagnetic responses

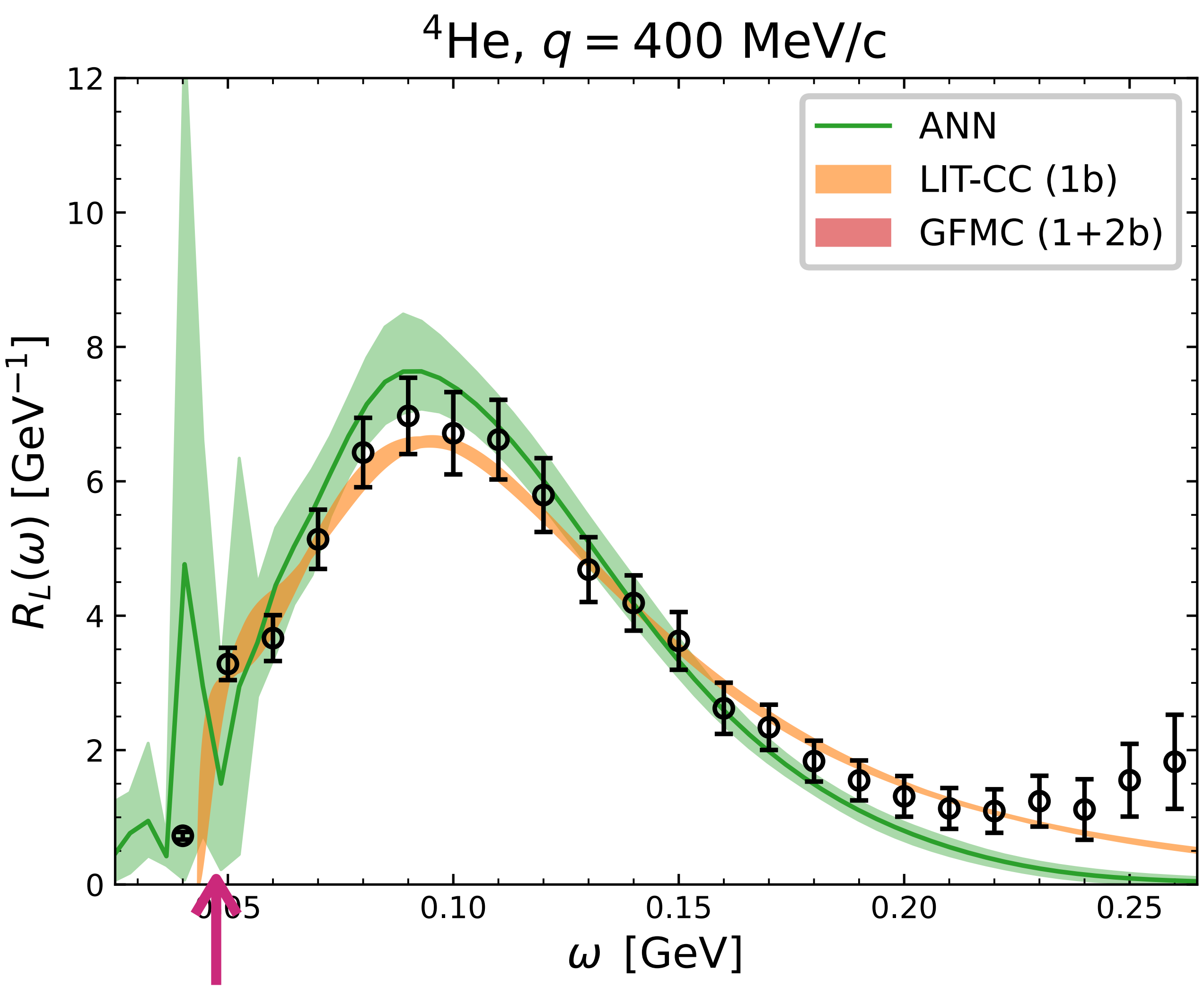

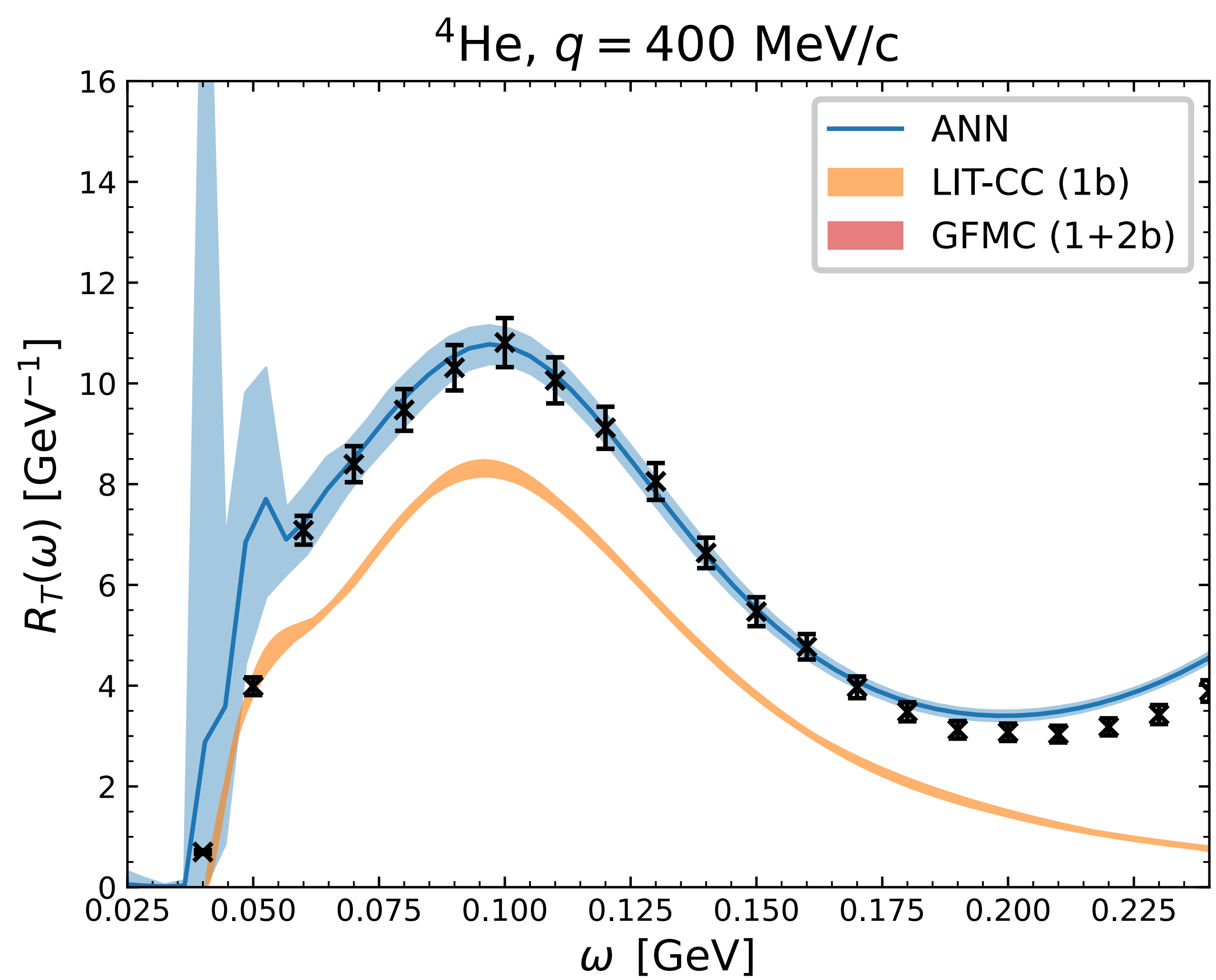

Low lying nuclear states

Contributions from elastic and low-lying inelastic transitions are explicitly removed from the GFMC responses and the Rosenbluth analysis, while they are present in the ANN curves

Noemi Rocco, nrocco@fnal.gov

Using Bayesian ANN for electron-nucleus scattering

J. Sobczyk, NR, A. Lovato, arxiv:2406.06292

Results: Electromagnetic responses

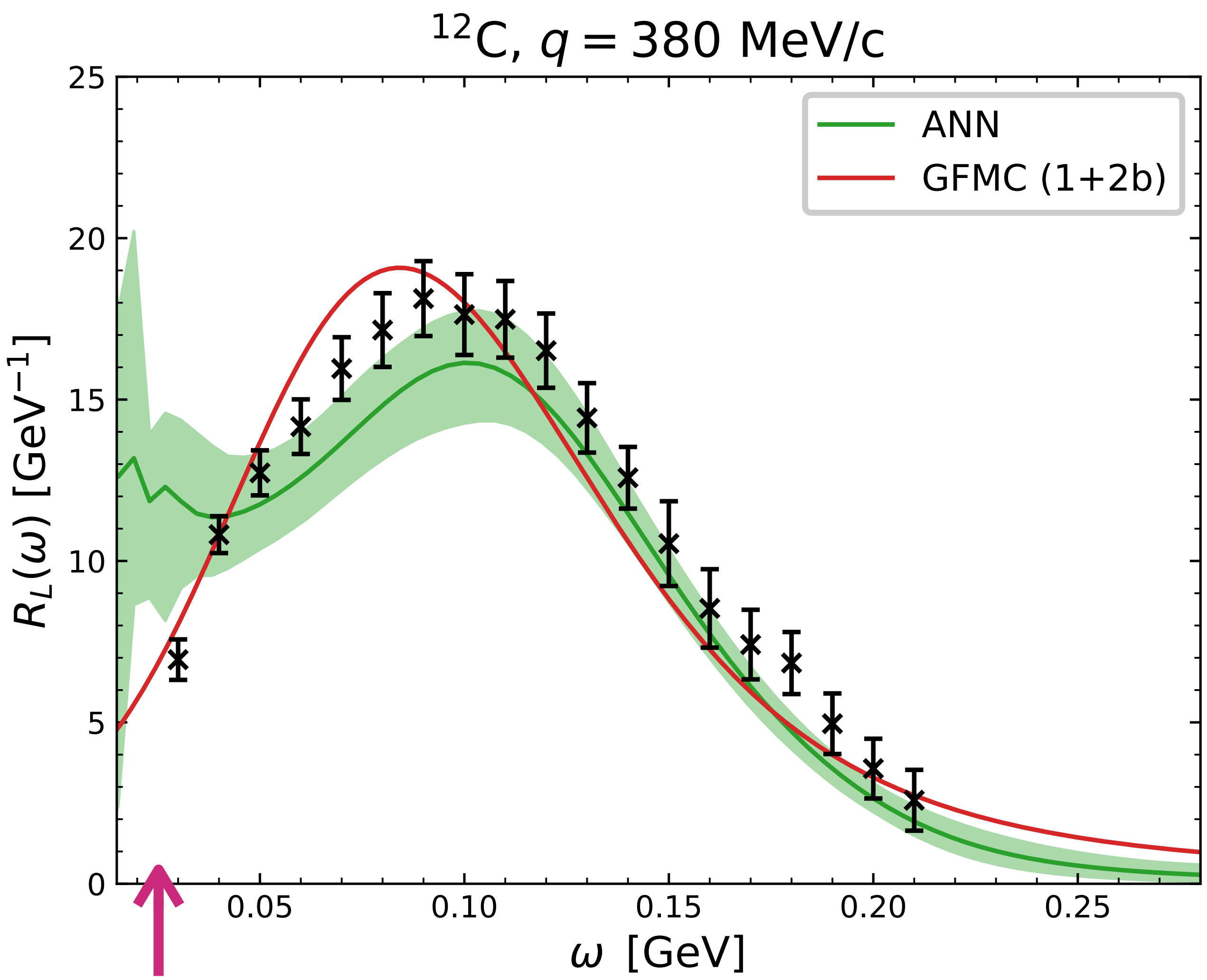

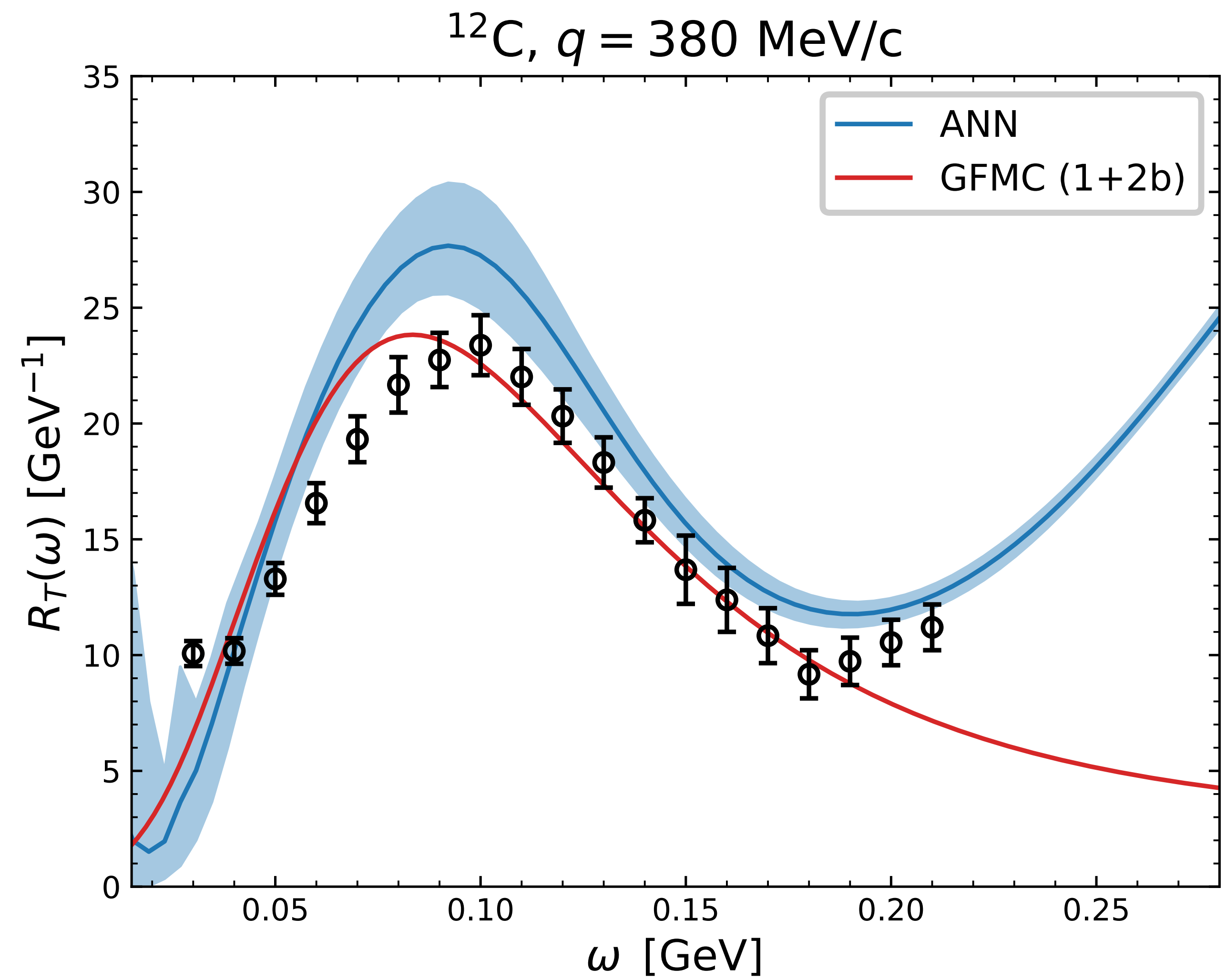

Low lying nuclear states

Contributions from elastic and low-lying inelastic transitions are explicitly removed from the GFMC responses and the Rosenbluth analysis, while they are present in the ANN curves

Noemi Rocco, nrocco@fnal.gov

Using Bayesian ANN for electron-nucleus scattering

J. Sobczyk, NR, A. Lovato, arxiv:2406.06292

Results: Electromagnetic responses

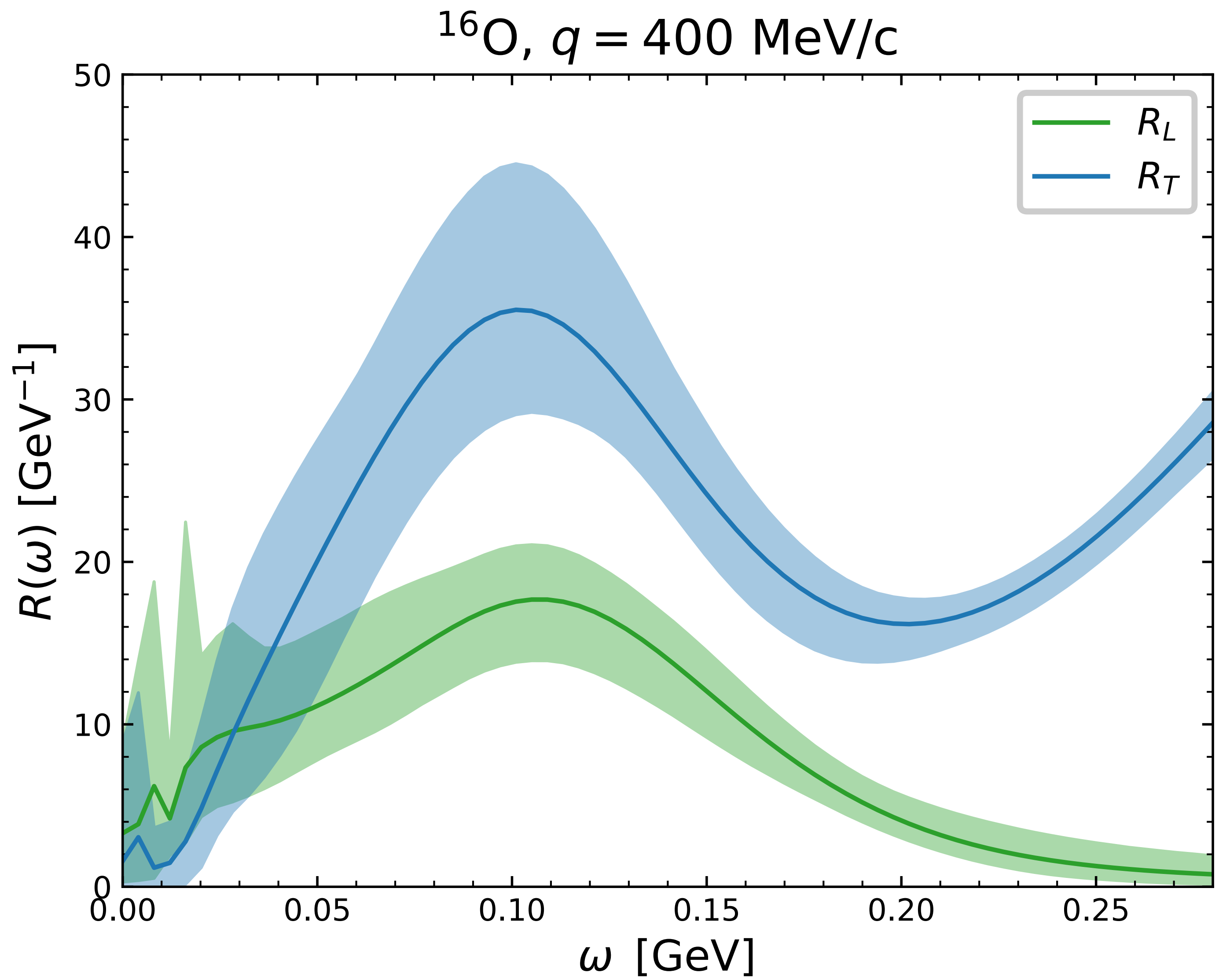

First separation of the longitudinal and transverse responses of ^{16}O. Large uncertainty bands reflect the **scarcity of inclusive cross section data.**

Noemi Rocco, nrocco@fnal.gov
Fermilab

Using Bayesian ANN for electron-nucleus scattering

J. Sobczyk, NR, A. Lovato, arxiv:2406.06292

Results: Electromagnetic responses

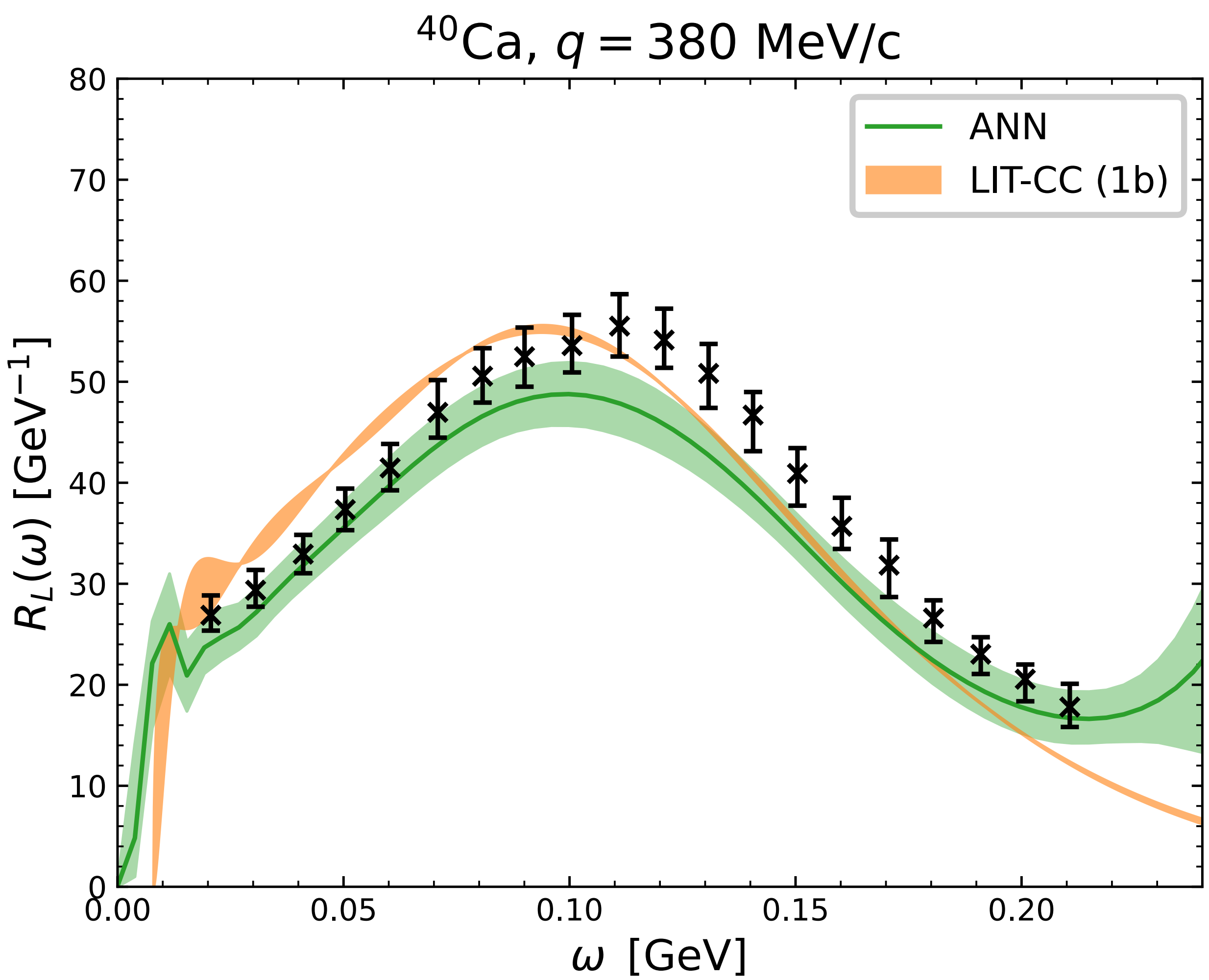

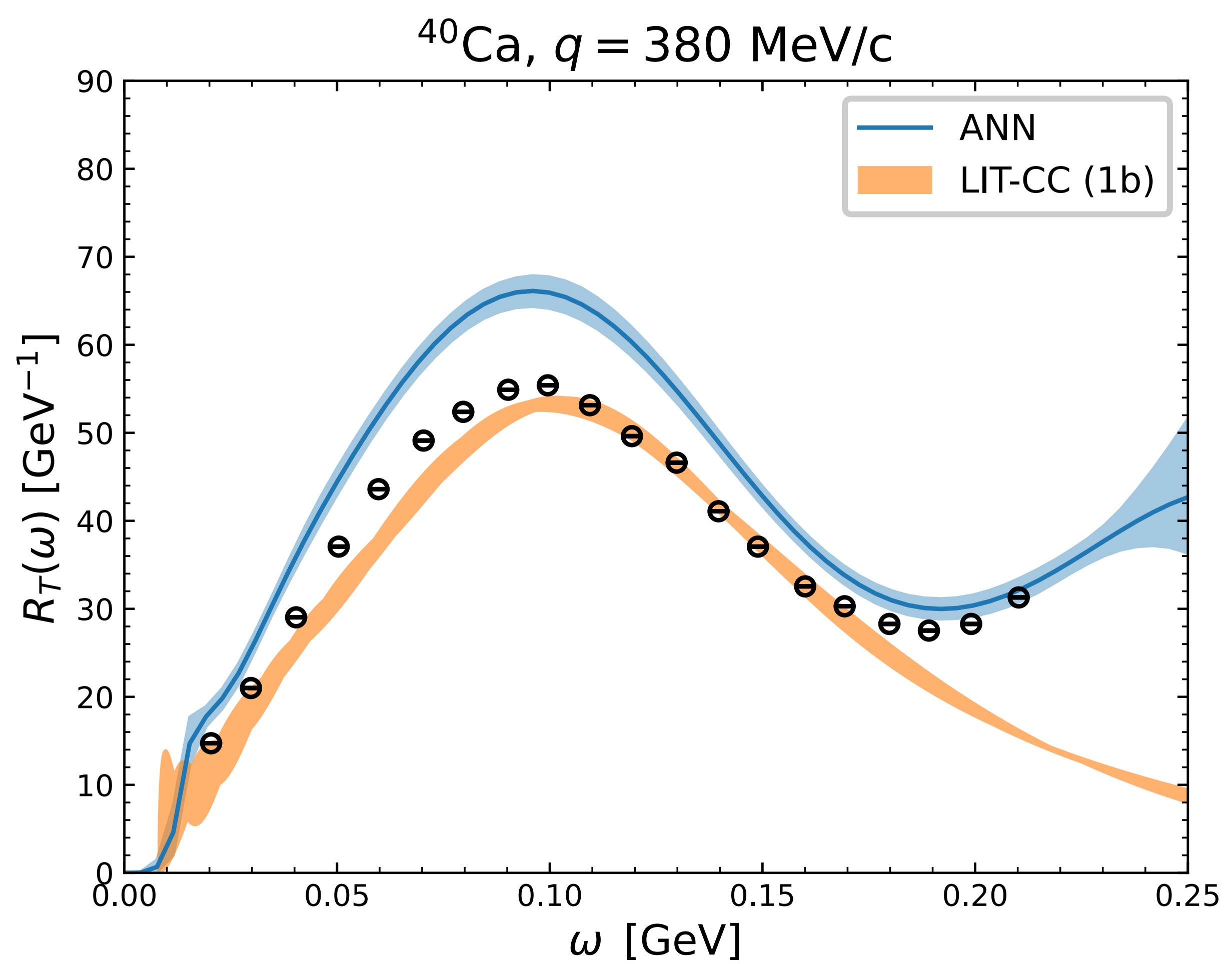

Note increasing error bars for large ω reflecting the scarcity of data for 40Ca in the high energy-momentum region. The net is learning from other nuclei in this region.

Dedicated discussion on the Rosenbluth separation carried out using two different experiments.

Conclusions

- Neutrino oscillation experiments are entering a new precision era

- To match these precision goals accurate predictions of neutrino cross sections are crucial

  Ab initio methods: almost exact results but limited in energy, fully inclusive

  Approaches based on factorization schemes are being further developed

- Uncertainty associated with the theory prediction of the hard interaction vertex needs to be assessed. Initial work has been carried out in this direction studying the dependence on:

  Form factors: one- and two-body currents, resonance/π production

  Error of factorizing the hard interaction vertex / using a non relativistic approach

- Combine state-of-the art neutrino-nucleus calculations with BSM theories is gaining momentum; UQ is very interesting (and challenging) in this case as well

Thank you for your attention!